Why equal-time abundance correlations alone do not identify ecological interactions

Akiva Goldberg and Nadav M. Shnerb*
Department of Physics, Bar-Ilan University, Ramat Gan 52900, Israel

(Received 19 May 2026; accepted 2 October 2026; published 16 November 2026)

Species similarity can imprint abundance fluctuations in two opposing ways: Similar species may respond similarly to environmental fluctuations, generating positive correlations, while stronger overlap in resource use enhances competition and generates negative correlations. In the absence of additional mechanistic information, the natural benchmark is therefore to match environmental-response similarity to competitive similarity. At this matched point, the two effects cancel exactly and equal-time interspecific correlations vanish, so nonzero correlations primarily measure departures from matching rather than niche overlap itself. Making resource dynamics explicit reveals two natural ways to break this cancellation. A temporal mismatch arises when environmental response is immediate but competitive feedback is delayed, allowing correlations to track niche overlap when the relevant timescale is known. A structural mismatch arises when fluctuations act through resources: Forcing then depends on yield, whereas competition depends on both yield and depletion, so correlations reflect yield-depletion mismatch. Equal-time correlations are therefore informative only relative to the mechanism that drives the system away from the matched benchmark.

DOI: 10.1103/kwr4-pzn2

I. INTRODUCTION

Time-resolved data on ecological communities have become increasingly abundant, and with them has come the hope of inferring community structure from fluctuations in species abundances. When two species rise and fall together, it is natural to suspect that they are similar. When they move in opposite directions, competition is the natural suspect. Accordingly, correlations between species abundances are often used as proxies for direct measures of ecological similarity and interaction, and these inferences are attracting growing interest, particularly in microbial communities [1–5]. Yet equal-time correlations, by themselves, do not identify the interaction structure. Interpreting them requires additional information about how the environment affects the species and about the timescales of the ecological response.

The root of the difficulty is that the same biological similarity can act in two opposing directions. Similar species tend to respond similarly to environmental fluctuations, causing their abundances to move together. On the other hand, the same species also tend to use similar resources and therefore to compete, pushing their abundances in opposite directions. The observed correlation is thus the outcome of a balance between a shared environmental response and competitive feedback. Its sign and magnitude are not determined by niche overlap alone.

In this paper, we examine this problem using standard Lotka-Volterra (LV) and consumer-resource (CR) models as analytic tools. We restrict attention to communities with a stable deterministic coexistence state and introduce environmental stochasticity, allowing either species growth rates or (when resources are explicit) resource growth rates to fluctuate randomly in time [6–8].

In the existing literature, the correlation structure of the noise is commonly imposed externally, and its consequences for abundance correlations are then examined. However, if the interaction matrix is interpreted as a measure of niche overlap [9,10], there is no reason to regard the two structures as independent: The same biological similarity that strengthens competition should, as a general tendency, also make species respond more similarly to environmental fluctuations. In the absence of additional mechanistic information, the matched choice is therefore the only benchmark that does not introduce an additional pairwise structure by hand. This is particularly relevant for the Lotka-Volterra description, whose appeal lies in its ability to capture generic properties of community dynamics across a broad class of more detailed ecological models [11].

However, precisely at this point the two opposing effects cancel: Equal-time interspecific correlations vanish. This cancellation is not merely a consequence of a linear approximation. For reciprocal interactions, it is known that the full nonlinear stationary distribution factorizes into independent single-species distributions [12], and we show below that this structure persists for nonreciprocal interactions as well. The matched point provides a genuine reference state rather than an accidental feature of the weak-noise approximation.

Accordingly, for Lotka-Volterra-like dynamics we show that interspecific correlations arise only from the response-competition mismatch, namely, the difference between similarity in environmental response and competitive similarity. Nonzero correlations signal a departure from the matched point, rather than directly revealing the interaction structure.

*Contact author: nadav.shnerb@gmail.com

Published by the American Physical Society under the terms of the Creative Commons Attribution 4.0 International license. Further distribution of this work must maintain attribution to the author(s) and the published article's title, journal citation, and DOI.

To infer interactions from equal-time correlations, one must supply an additional assumption or independent information, about the structure of the environmental response.

A less schematic picture emerges once the dynamics of the resources themselves are taken into account. Making the resource degrees of freedom explicit reveals two physically distinct and biologically plausible mechanisms that can generate a mismatch between environmental response and competition.

The first mechanism is temporal mismatch: The environmental response can act directly on the consumers, whereas competition is transmitted through the resource pool and therefore acts with a delay. When the direct environmental response is matched to competitive similarity, sufficiently slow resource dynamics break the cancellation and allow the correlations to track niche overlap.

The second mechanism is structural mismatch. When environmental fluctuations act through the resources [4,13], the structure of the forcing inherited by the consumers need not be identical to the structure of competition. The former is determined by what consumers gain from the resources, whereas the latter also depends on what they deplete. When yield and depletion differ only by a common conversion factor, as assumed in many consumer-resource (CR) models [14], the two structures remain matched and the correlations vanish. If, in contrast, yield and depletion are misaligned, nonzero correlations appear. In that case, however, the correlations reflect the yield-depletion mismatch (YDM) [13] rather than niche overlap itself.

In real communities, we generally do not know independently the route by which environmental variability enters the system, how similar the environmental responses of different species are, or the timescale of competitive feedback. As a result, the same interaction matrix can generate very different correlation patterns, while the same correlation pattern can be compatible with different interaction structures. Their interpretation is therefore intrinsically conditional on mechanistic information that is not contained in the equal-time correlation matrix itself.

II. FRAMEWORK: ONE INFERENCE PROBLEM, TWO LEVELS OF DESCRIPTION

Throughout this paper, we describe the same ecological system at two levels of resolution: an explicit CR description and its effective LV reduction. The former retains the resource dynamics explicitly, whereas the latter represents their net effect through an interaction matrix.

Consider a community of S consumer species competing for Q resources. The abundance of consumer i is $n_i(t)$ and the biomass of resource k is $R_k(t)$. Consumer growth is driven by resource uptake, while each resource grows logistically in the absence of consumers and is depleted through consumption:

$$\frac{dn_i(t)}{dt} = -n_i + n_i \sum_{k=1}^{Q} \gamma_{ik} R_k,$$
$$\tau_R \frac{dR_k(t)}{dt} = R_k - R_k^2 - R_k \sum_{i=1}^{S} \lambda_{ki} n_i. \tag{1}$$

Here, γ_{ik}, the (i,k) entry of the $S \times Q$ matrix Γ, quantifies *yield*: the increase in the growth rate of consumer i per unit of resource k. λ_{ki}, the (k,i) entry of the $Q \times S$ matrix Λ, quantifies *depletion*: the per-capita rate at which consumer i removes resource k. The parameter τ_R sets the resource-response timescale relative to the consumer timescale. The fast-resource regime corresponds to $\tau_R \ll 1$.

The CR formulation keeps yield and depletion as distinct quantities. In traditional consumer-resource models, they are often tied together by assuming that, for each resource,

$$\gamma_{ik} = c_k \lambda_{ki}, \tag{2}$$

where c_k is a conversion factor associated with resource k [14]. We do not impose this relation: Yield and depletion may be misaligned because the benefit obtained from a resource need not be proportional to the amount removed, for example, because of variation in conversion efficiency, wasteful uptake, cross feeding, or metabolic by-products [15–25].

In the limit $\tau_R \to 0$, the resource variables may be adiabatically eliminated, yielding the Lotka-Volterra description

$$\frac{dn_i}{dt} = n_i \left(r_i - \sum_j \alpha_{ij} n_j \right), \quad r_i = \sum_k \gamma_{ik} - 1, \tag{3}$$

with the effective interaction matrix

$$\boldsymbol{\alpha} = \Gamma \Lambda. \tag{4}$$

For most of the paper, we restrict attention, for convenience, to communities with uniform intrinsic growth rates $r_i = 1$ and normalize the self-interactions to $\alpha_{ii} = 1$. In the CR realizations, the first condition is imposed by constraining the rows of Γ to satisfy $\sum_k \gamma_{ik} = 2$. Pairs (Γ, Λ) that reproduce a prescribed interaction matrix while satisfying the ecological constraints are generated as described in Appendix A. With these conventions, Eq. (3) takes the familiar form

$$\frac{dn_i}{dt} = n_i \left(1 - n_i - \sum_{j \neq i} \alpha_{ij} n_j \right), \tag{5}$$

widely used in the analysis of competitive Lotka-Volterra communities [11,13,26–28]. The restrictions $r_i = 1$ and $\alpha_{ii} = 1$ are adopted only for convenience of presentation. The corresponding results for general r_i and α_{ii} are given in Appendix C.

With the diagonal normalized to unity, α_{ij} may be interpreted as an effective measure of niche overlap between consumers i and j [9,10,29]. When $\boldsymbol{\alpha}$ is not symmetric, we distinguish its symmetric and antisymmetric parts,

$$\boldsymbol{\alpha}_S = \frac{\boldsymbol{\alpha} + \boldsymbol{\alpha}^T}{2}, \quad \boldsymbol{\alpha}_A = \frac{\boldsymbol{\alpha} - \boldsymbol{\alpha}^T}{2}. \tag{6}$$

The symmetric part carries the pairwise competitive similarity relevant to niche overlap, whereas the antisymmetric part describes directional asymmetry, or fitness differences, in the interactions. The distinction will become important below because a noise covariance is necessarily symmetric and can be matched only to $\boldsymbol{\alpha}_S$.

Equation (4) also shows what is lost in the LV reduction. Yield and depletion survive only through the product $\Gamma\Lambda$, so

different pairs (Γ, Λ) can generate the same interaction matrix, while the resource timescale τ_R disappears entirely. These details do not affect the deterministic equilibrium, which is fixed by $\boldsymbol{\alpha}$, but they can strongly affect fluctuations about it [13]. The reduction therefore removes two pieces of mechanistic information that will reappear below as distinct sources of ambiguity in abundance correlations: the resource-response timescale and the separate yield and depletion structures.

III. EQUAL-TIME CORRELATIONS REQUIRE A MODEL OF THE ENVIRONMENTAL FORCING

A. The identifiability problem

We now turn to the central inference problem. Even within the Lotka-Volterra description, abundance correlations are not determined by the interaction matrix alone. They arise jointly from the deterministic interactions and from the structure of the environmental forcing. Accordingly, equal-time abundance data contain three distinct objects: the interaction matrix, the covariance of the environmental response, and the resulting covariance of the abundance fluctuations. The last of these is observed, while the first two are generally unknown. Consequently, equal-time correlations cannot identify the interactions unless additional information about the environmental forcing is supplied.

To make this nonidentifiability explicit, we introduce environmental variability at the Lotka-Volterra level as a fluctuating contribution to the species growth rates,

$$\frac{dn_i}{dt} = n_i\left(1 - n_i - \sum_{j\neq i}\alpha_{ij}n_j\right) + \sigma_e\, n_i\, \eta_i(t), \tag{7}$$

where $\langle \eta_i(t)\rangle = 0$ and

$$\langle \eta_i(t)\eta_j(t')\rangle = C^{(\eta)}_{ij}\,\delta(t-t'). \tag{8}$$

We take $C^{(\eta)}_{ii} = 1$, so that σ_e sets the overall noise amplitude while $C^{(\eta)}$ specifies the correlation structure of the environmental response. We use the Stratonovich convention throughout. The Itô convention shifts the deterministic drift but does not alter the identifiability argument or the conclusions below, as discussed in Appendix C.

We assume that the deterministic dynamics support a stable coexistence state $\bar{\mathbf{n}}$, satisfying $\boldsymbol{\alpha}\bar{\mathbf{n}} = \mathbf{1}$, and define $N = \mathrm{diag}(\bar{n}_1, \ldots, \bar{n}_S)$. Linearizing Eq. (7) about this state, the fluctuations $\delta n_i = n_i - \bar{n}_i$ obey a multivariate Ornstein-Uhlenbeck process with drift matrix

$$J = -N\boldsymbol{\alpha} \tag{9}$$

and noise covariance

$$D = \sigma_e^2\, NC^{(\eta)}N. \tag{10}$$

The stationary abundance covariance $\Sigma_{ij} = \langle \delta n_i \delta n_j\rangle$ therefore satisfies the Lyapunov equation

$$J\Sigma + \Sigma J^T = -D, \tag{11}$$

and the corresponding equal-time abundance correlations are $\rho_{ij} = \Sigma_{ij}/\sqrt{\Sigma_{ii}\Sigma_{jj}}$.

Equation (11) makes the identifiability problem explicit. The observed covariance Σ is determined jointly by the deterministic drift, through J and hence $\boldsymbol{\alpha}$, and by the environmental forcing, through D and hence $C^{(\eta)}$. Therefore, Σ alone does not determine the interaction matrix. Indeed, for any candidate interaction matrix that supports a stable coexistence state, Eq. (11) specifies the noise covariance required to reproduce a given target covariance Σ^*,

$$D(\boldsymbol{\alpha}, \Sigma^*) = -(J\Sigma^* + \Sigma^* J^T), \quad C^{(\eta)} = \sigma_e^{-2}N^{-1}DN^{-1}. \tag{12}$$

Whenever the resulting $C^{(\eta)}$ is an admissible covariance matrix, the same equal-time abundance covariance is compatible with that alternative interaction matrix. Explicit constructions showing that this occurs for very different, and even oppositely ordered, interaction matrices are given in Appendix D.

Accordingly, measurement of Σ alone does not determine J, and hence does not determine the interaction matrix $\boldsymbol{\alpha}$: The same abundance covariance can arise from different drift matrices when they are accompanied by different environmental covariances. To proceed, one must therefore supply additional information about the forcing.

B. Matched noise

In the absence of such additional insight, the only natural biological benchmark is the one that introduces no new pairwise structure beyond that already present in the interactions. If ecological similarity makes two species compete for the same resources, it is natural to take the same similarity to make them respond similarly to environmental fluctuations. Since a covariance matrix is symmetric, the corresponding matched condition is

$$C^{(\eta)} = \boldsymbol{\alpha}_S, \tag{13}$$

where $\boldsymbol{\alpha}_S$ is defined in Eq. (6).

The consequence of this benchmark follows directly from the Lyapunov equation. Write the stationary covariance as

$$\Sigma = \frac{\sigma_e^2}{2}N + NYN, \tag{14}$$

where Y contains the departure from the diagonal covariance expected at the matched point. Substituting Eq. (14) into Eq. (11), using $J = -N\boldsymbol{\alpha}$ and $D = \sigma_e^2 NC^{(\eta)}N$, gives

$$\boldsymbol{\alpha}NY + YN\boldsymbol{\alpha}^T = \sigma_e^2(C^{(\eta)} - \boldsymbol{\alpha}_S). \tag{15}$$

At the matched point [Eq. (13)], the right-hand side of Eq. (15) vanishes. The resulting homogeneous Sylvester equation has a unique solution because the coexistence state is linearly stable (Appendix B). Since $Y = 0$ is a solution, it is the only one. Hence,

$$\Sigma = \frac{\sigma_e^2}{2}N, \quad \rho_{ij} = 0 \quad (i \neq j). \tag{16}$$

Thus, within the linearized Lotka-Volterra description, matching environmental response to competitive similarity removes all equal-time interspecific correlations, for arbitrary species number, interaction heterogeneity, and nonreciprocal interactions.

This cancellation is not merely a consequence of linearization. At the matched point, the full nonlinear stationary

distribution factorizes into independent single-species distributions, so that all equal-time interspecific dependence vanishes even for nonreciprocal interactions, where the stationary state may carry a nonzero probability current. The nonlinear results are derived in Appendix C.

C. Correlations reflect mismatch, not interaction—the two-species case

Equation (15) also identifies what produces nonzero correlations away from the matched point. It therefore motivates defining the response-competition mismatch

$$\boldsymbol{\beta} \equiv C^{(\eta)} - \boldsymbol{\alpha}_S. \tag{17}$$

Equation (15) shows more generally what the equal-time correlations measure away from the matched point. Every departure of Σ from the diagonal baseline $(\sigma_e^2/2)N$ is driven by the mismatch $\boldsymbol{\beta}$. The interaction matrix $\boldsymbol{\alpha}$ still enters the left-hand side and therefore determines how a given mismatch is propagated through the community, but it does not generate off-diagonal covariance by itself. In this sense, the response-competition mismatch is the primary determinant of equal-time abundance correlations, while the interaction matrix contributes only secondarily by shaping how that mismatch is propagated.

The mechanism is already transparent for two species. For symmetric competition, $\alpha_{12} = \alpha_{21} = \alpha$, Eq. (15) can be solved in closed form, giving

$$\rho_{12} = \frac{C_{12}^{(\eta)} - \alpha}{1 - \alpha C_{12}^{(\eta)}} = \frac{\beta_{12}}{1 - \alpha C_{12}^{(\eta)}}. \tag{18}$$

Competition and shared environmental response act in opposite directions: The former anticorrelates the abundances, whereas the latter synchronizes them. Their effects cancel exactly at the matched point $C_{12}^{(\eta)} = \alpha$. Away from that point, the sign of the abundance correlation is set by the sign of the mismatch, while the interaction strength enters through the denominator and modulates the response.

Figure 1 illustrates this result by taking $C_{12}^{(\eta)} = b\alpha$. In this case,

$$\rho_{12} = \frac{(b-1)\alpha}{1 - b\alpha^2}. \tag{19}$$

For $b < 1$, competition dominates the shared environmental response and the abundances are anticorrelated. For $b > 1$, the shared response dominates and the correlation is positive. At the matched value $b = 1$, the correlation vanishes for every value of the niche overlap. Thus, even in the simplest two-species system the sign and magnitude of the abundance correlation cannot be interpreted as a direct measure of competition without knowing how strongly the two species share the environmental forcing.

D. Correlations reflect mismatch, not interaction — diverse communities

The same conclusion extends beyond two species. To see this, write the interaction matrix as

$$\boldsymbol{\alpha} = \bar{\boldsymbol{\alpha}} + \delta\boldsymbol{\alpha}, \tag{20}$$

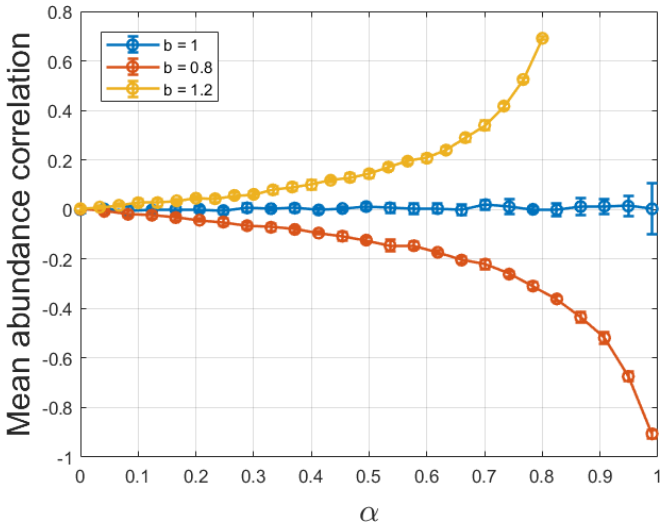


FIG. 1. Two species: The abundance correlation is governed by the response-competition mismatch. Stochastic Lotka-Volterra dynamics [Eq. (7)] for $S = 2$, with symmetric competition $\alpha_{12} = \alpha_{21} = \alpha$ and environmental correlation $C_{12}^{(\eta)} = b\alpha$. Solid curves show the closed-form solution of the linearized Lyapunov equation [Eq. (18)], which in this case becomes $\rho_{12} = (b-1)\alpha/(1-b\alpha^2)$. The mismatch $\beta_{12} = (b-1)\alpha$ sets the sign and provides the source of the correlation, while the interaction strength enters through the propagator in the denominator. Symbols are direct Stratonovich simulations of Eq. (7) with $\sigma_e = 0.05$. At the matched benchmark, $b = 1$, the correlation vanishes for every value of the niche overlap. For $b < 1$, competition dominates and the correlation is negative, whereas for $b > 1$, the shared environmental response dominates and the correlation is positive.

where $\bar{\boldsymbol{\alpha}}$ has unit diagonal and a common off-diagonal interaction μ, while $\delta\boldsymbol{\alpha}$ contains the pair-to-pair variation one would like to infer. Near the matched point, Eq. (15) implies $Y = O(\boldsymbol{\beta})$. The heterogeneous part $\delta\boldsymbol{\alpha}$ therefore enters the left-hand side only multiplied by Y, and contributes at order $O(\delta\boldsymbol{\alpha} \cdot \boldsymbol{\beta})$. To leading order in both the mismatch and the interaction heterogeneity,

$$\bar{K}Y + Y\bar{K}^T = \sigma_e^2\boldsymbol{\beta}, \quad \bar{K} = \bar{\boldsymbol{\alpha}}\bar{N}. \tag{21}$$

Thus, the pairwise heterogeneity of the niche overlaps is absent from the leading-order source of the abundance correlations. It reappears only at higher order, through the way the community propagates a preexisting mismatch.

In a diverse community, the ambiguity does not disappear. For a homogeneous background interaction matrix, the leading-order solution of Eq. (21) gives, at large S,

$$\rho_{ij} \simeq \frac{\tilde{\beta}_{ij}}{1-\mu}, \tag{22}$$

where $\tilde{\beta}_{ij}$ is the centered response-competition mismatch (see Appendix E). Thus, the pairwise abundance correlations remain of order unity and continue to reflect the mismatch rather than the pair-to-pair variation in niche overlap. This behavior is illustrated in Fig. 2: The correlations collapse onto the prediction based on the centered mismatch, while showing essentially no pairwise relation with α_{ij}.

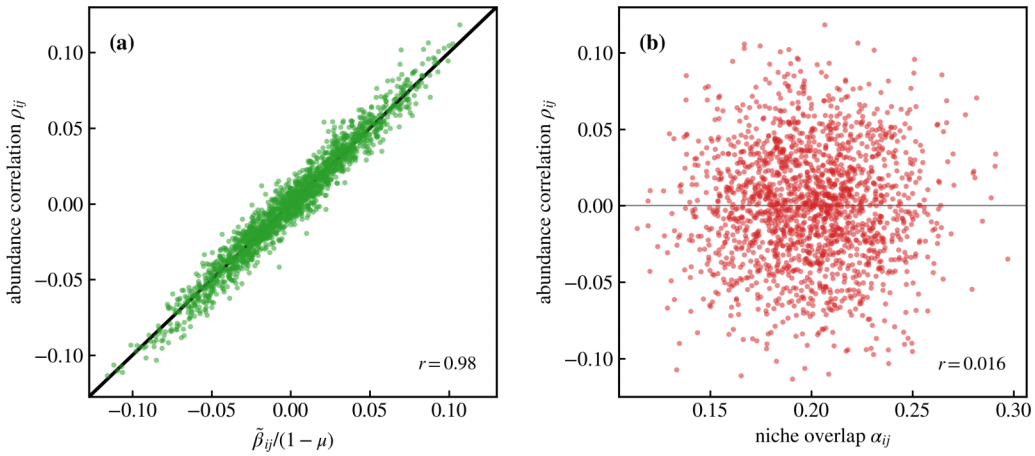


FIG. 2. In a diverse community, abundance correlations follow the response-competition mismatch rather than pairwise niche overlap. A community of $S = 60$ species with heterogeneous symmetric interactions $\alpha_{ij} = \mu + \delta\alpha_{ij}$, with $\mu = 0.2$, and environmental forcing $C^{(\eta)} = \boldsymbol{\alpha}_S + \boldsymbol{\beta}$. The interaction heterogeneity $\delta\alpha_{ij}$ and the mismatch β_{ij} are drawn independently with the same standard deviation $\sigma = 0.03$. Each point represents one of the 1770 species pairs, and the correlations are obtained by solving the linearized Lyapunov equation. (a) ρ_{ij} vs the large-S prediction $\tilde{\beta}_{ij}/(1-\mu)$. (b) The same correlations vs the actual pairwise niche overlap α_{ij}. The correlations closely follow the centered mismatch, whereas no corresponding pairwise relation with niche overlap is visible.

Increasing community size therefore does not resolve the identifiability problem. Equal-time correlations can become informative only when additional information is supplied about the structure or mechanism of the environmental forcing. In the following section, we analyze two mechanistic insights that emerge at the consumer-resource level.

IV. HOW MISMATCH ARISES NATURALLY IN CONSUMER-RESOURCE DYNAMICS

The Lotka-Volterra analysis identifies the response-competition mismatch as the source of nonzero equal-time correlations, but it does not by itself provide a benchmark for the size or origin of that mismatch. At the LV level, the interaction matrix $\boldsymbol{\alpha}$ is the only internal description of ecological similarity, while the environmental-response covariance $C^{(\eta)}$ is specified externally. The matched condition $C^{(\eta)} = \boldsymbol{\alpha}_S$ therefore provides a natural reference point, but once the two structures differ the LV model contains no additional mechanistic information with which to interpret that difference.

Accordingly, to gain insight into the mechanistic origins of the mismatch in realistic community dynamics, we turn to the consumer-resource system, whose deterministic dynamics still support a stable coexistence state but which is now subject to environmental stochasticity,

$$\frac{dn_i}{dt} = -n_i + n_i \sum_{k=1}^{Q} \gamma_{ik} R_k + \sigma_c\, \xi_i(t)\, n_i, \tag{23a}$$

$$\tau_R \frac{dR_k}{dt} = R_k - R_k^2 - R_k \sum_{i=1}^{S} \lambda_{ki} n_i + \sigma_r\, \zeta_k(t)\, R_k. \tag{23b}$$

The environment can now act through two distinct channels. Direct consumer forcing has covariance

$$\langle \xi_i(t)\xi_j(t')\rangle = C_{ij}^{(\xi)}\, \delta(t-t'), \quad C_{ii}^{(\xi)} = 1, \tag{24}$$

whereas resource fluctuations are taken to be independent,

$$\langle \zeta_k(t)\zeta_l(t')\rangle = \delta_{kl}\, \delta(t-t'). \tag{25}$$

The two channels can be isolated separately: $\sigma_r = 0$ leaves only direct consumer forcing, while $\sigma_c = 0$ leaves only resource-mediated forcing. In the deterministic fast-resource limit, Eqs. (23) reduce to the Lotka-Volterra system of Sec. II, with $\boldsymbol{\alpha} = \Gamma\Lambda$.

The consumer-resource description restores precisely the information that was lost in the LV reduction. In particular, it supplies two independent physical handles on the mismatch. The first is temporal: Environmental forcing and competitive feedback need not act on the same timescale, because competition is mediated by resources. The second is structural: When environmental fluctuations act through the resources, the covariance inherited by the consumers depends on the yield matrix Γ, whereas competition depends on the product $\Gamma\Lambda$. The relation between yield and depletion therefore provides an additional benchmark for whether forcing and competition should be expected to match.

We examine these two mechanisms in turn. First, we consider temporal mismatch, where a finite resource-response time delays competition relative to the shared environmental response. We then consider structural mismatch, where forcing and competition act on the same effective timescale but differ because yield and depletion are not aligned.

A. Temporal mismatch: delayed competitive feedback

The first source of mismatch restored by the consumer-resource description is temporal. In the effective Lotka-Volterra model, environmental response and competitive feedback act instantaneously. With explicit resources, however, competition is transmitted through the resource pool and may therefore lag a direct environmental response of the consumers. The resource timescale τ_R, which disappeared under the LV reduction, provides a physical measure of this delay.

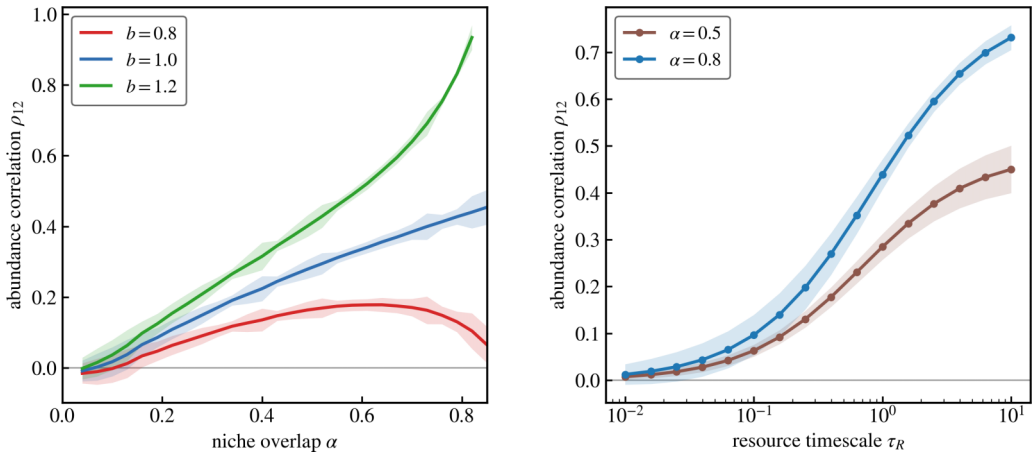


FIG. 3. Temporal mismatch breaks the matched cancellation. Abundance correlation between two consumers in the stochastic consumer-resource system [Eq. (23)], with environmental forcing acting directly on the consumers ($\sigma_r = 0$, $\sigma_c = 0.05$), $S = 2$, and $Q = 3$. Solid curves are means over 100 accepted (Γ, Λ) realizations that reproduce the same niche-overlap matrix; shaded bands show one standard deviation across realizations. (a) Correlation vs niche overlap α at $\tau_R = 1$, with $C_{ij}^{(\xi)} = b\,\alpha_{ij}$. At the matched benchmark $b = 1$, for which the instantaneous Lotka-Volterra description gives $\rho_{ij} = 0$ for every overlap (Fig. 1), the correlation is positive and increases with α because competitive feedback is delayed by the resource dynamics. For $b \neq 1$, the preexisting response-competition mismatch modifies this relation. The nonmonotonic behavior at $b = 0.8$ reflects a competition between two contributions of opposite sign: The delayed competitive feedback exposes the shared environmental response, a positive contribution that grows with α but remains bounded, while the instantaneous mismatch contribution [Eq. (19)] is negative for $b < 1$ and is amplified as $(b-1)\alpha/(1-b\alpha^2)$, so without delay it approaches -1 as $\alpha \to 1$. (b) Correlation at $b = 1$ as the resource timescale τ_R is varied over three decades, for two values of the niche overlap. As $\tau_R \to 0$, the resources become slaved to the consumers, the effective dynamics approaches the matched stochastic Lotka-Volterra system, and the correlation tends to zero. The nonzero signal is therefore generated by temporal mismatch rather than by the consumer-resource description itself.

To isolate temporal mismatch, we first set $\sigma_r = 0$, so that the environment acts directly on the consumers, and impose the same matched benchmark used at the LV level,

$$C^{(\xi)} = \boldsymbol{\alpha}_S, \quad \boldsymbol{\alpha} = \Gamma\Lambda. \tag{26}$$

At the LV level, this condition gives zero equal-time interspecific correlations. With finite τ_R, however, the two effects no longer act simultaneously: The shared environmental response is immediate, whereas competition is transmitted through the resource dynamics. The cancellation is therefore incomplete. To gain analytical insight into this mechanism, we consider a simplified tractable limit in which $\boldsymbol{\alpha}$ is symmetric and the resource equilibria are uniform. In this case, the abundance correlations can be obtained in closed form (Appendix F),

$$\rho_{ij} = \alpha_{ij}\sqrt{\frac{\theta_i}{1+\theta_i}}\sqrt{\frac{\theta_j}{1+\theta_j}}, \quad (i \neq j), \tag{27}$$

where $\theta_i \equiv \tau_R\,\bar{n}_i$. Clearly, the interspecific correlations vanish at the limit $\tau_R \to 0$, where the consumer-resource dynamics converges to the Lotka-Volterra case.

The general behavior of correlations in such a system is demonstrated in Fig. 3(a). At the matched benchmark, $b = 1$, the abundance correlation grows with α, in qualitative agreement with the analytical benchmark [Eq. (27)]. If the direct environmental covariance does not match $\boldsymbol{\alpha}_S$, the preexisting response-competition mismatch remains and can distort, or even render nonmonotonic, the relation between ρ_{ij} and α_{ij}, as seen for $b \neq 1$. As $\tau_R \to 0$, the resources become slaved to the consumers, the effective dynamics approaches the stochastic Lotka-Volterra system with $\boldsymbol{\beta} = 0$, and the cancellation is restored, as demonstrated in Fig. 3(b).

Thus, when competitive feedback is sufficiently delayed relative to a shared direct response, equal-time correlations can track niche overlap. This provides a possible mechanism for a decay of abundance correlations with phylogenetic distance, if phylogenetic distance itself tracks niche overlap, as reported by Sireci *et al.* [2].

That interpretation, however, requires information that is not contained in the equal-time correlation matrix itself: One must know that competitive feedback is appreciably delayed relative to the direct environmental response, and one must know how closely that direct response covariance follows the niche-overlap matrix. Temporal structure can therefore make abundance correlations informative, but only once the relevant timescale and forcing mechanism are supplied independently, or at least constrained by an informed estimate.

B. Structural mismatch: yield–depletion misalignment

The second source of mismatch that may appear naturally in consumer-resource systems is structural. We now set $\sigma_c = 0$ and let the environment act only through fluctuations of the resources. Unlike direct consumer forcing, the covariance experienced by the consumers is then not imposed externally. It is generated by their resource-use traits.

This structure is most transparent in the fast-resource reduction. Adiabatic elimination of the fluctuating resources gives an effective stochastic Lotka-Volterra system (Appendix G) with

$$\boldsymbol{\alpha} = \Gamma\Lambda, \quad C^{\text{eff}} = \sigma_r^2\,\Gamma\Gamma^T. \tag{28}$$

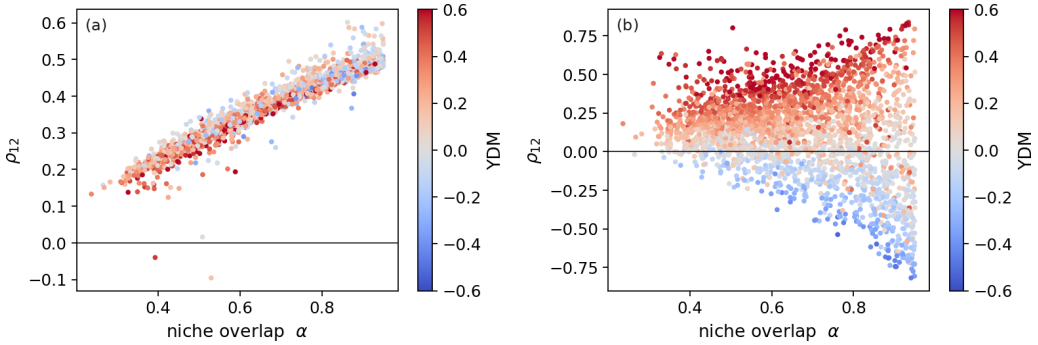


FIG. 4. Structural mismatch destroys a unique relation between correlation and niche overlap. Each point is one accepted (Γ, Λ) realization of a two-consumer, three-resource community with $\tau_R = 1$; color denotes the YDM of Ref. [13]. (a) Direct consumer forcing ($\sigma_r = 0$, $\sigma_c = 0.05$, $C^{(\xi)} = \boldsymbol{\alpha}_S$). The correlations are organized primarily by the niche overlap, reproducing the retardation regime of Sec. IV A, while the yield-depletion mismatch does not order the points. (b) Resource-mediated forcing ($\sigma_r = 0.05$, $\sigma_c = 0$). The collapse with niche overlap is lost. At fixed α, the abundance correlation can have either sign, while the yield-depletion mismatch strongly orders the cloud. Communities with the same effective interaction strength, and therefore the same niche overlap at the LV level, can be positively correlated, uncorrelated, or negatively correlated because they differ in the underlying relation between yield and depletion.

The two matrices therefore retain different pieces of the underlying consumer-resource structure. Competition depends on both yield and depletion, through $\Gamma\Lambda$, whereas the environmental covariance inherited by the consumers depends on yield alone, through $\Gamma\Gamma^T$. Accordingly, in that case we may find a structural mismatch that generates nontrivial interspecific correlations.

To turn this intuition into a systematic mathematical result, we must first address some technicalities. In contrast to the normalized $C^{(\eta)}$ used above, C^{eff} is a full covariance matrix whose diagonal need not be uniform. Let

$$H = \text{diag}\left(C^{\text{eff}}_{11}, \ldots, C^{\text{eff}}_{SS}\right). \tag{29}$$

For species-dependent forcing amplitudes, the covariance that exactly matches the interaction structure is

$$Z = \tfrac{1}{2}(\boldsymbol{\alpha} H + H\boldsymbol{\alpha}^T), \tag{30}$$

as derived in Appendix C. The structural analog of the response-competition mismatch is, thus, the departure of the inherited resource covariance from this matched covariance,

$$\Delta^{\text{eff}} \equiv C^{\text{eff}} - Z. \tag{31}$$

When the forcing amplitudes are common, $H \propto I$, this reduces, after factoring out the common amplitude, to the mismatch $C^{(\eta)} - \boldsymbol{\alpha}_S$ introduced above. The exact normalized form for nonuniform amplitudes is given in Appendix H.

We can now identify the appropriate biological benchmark for the matched point, at which equal-time correlations vanish, when environmental stochasticity enters through the resources. Consider the globally proportional case

$$\Lambda = c\,\Gamma^T. \tag{32}$$

Then,

$$\boldsymbol{\alpha} = c\,\Gamma\Gamma^T, \quad C^{\text{eff}} = \sigma_r^2\,\Gamma\Gamma^T = \frac{\sigma_r^2}{c}\,\boldsymbol{\alpha}. \tag{33}$$

Because $\alpha_{ii} = 1$, the diagonal of $\Gamma\Gamma^T$ is then uniform, so $H = (\sigma_r^2/c)I$. Consequently, $C^{\text{eff}} = Z$: The environmental covariance inherited through the resources is exactly the covariance required for cancellation. Resource fluctuations, however strong, generate no equal-time interspecific correlations in this proportional benchmark.

Once yield and depletion are no longer aligned, the two structures separate. The interaction matrix still contains only the product $\Gamma\Lambda$, while the inherited forcing contains $\Gamma\Gamma^T$. Two consumer-resource systems can have the same niche-overlap matrix $\boldsymbol{\alpha}$ but different structural mismatches and hence different abundance correlations. The resulting signal is not a direct measure of niche overlap. Rather, it reflects information about the relation between what consumers gain from the resources and what they remove from them.

Figure 4 makes this distinction explicit. Under direct consumer forcing [panel (a)], the matched forcing structure is imposed and finite resource retardation produces a correlation that is largely organized by niche overlap, as in Sec. IV A. Under resource-mediated forcing [panel (b)], no consumer-level covariance is imposed. Communities with the same α then exhibit correlations of either sign, and the cloud is instead ordered by the YDM, introduced in Ref. [13]. The quantity YDM is not identical to Δ^{eff}: The latter is the dynamical mismatch entering the covariance problem, whereas YDM is a geometric measure of the relative similarity of the yield and depletion profiles. In the exactly solvable two-species example of Appendix H, however, the two change sign at the same points and provide the same qualitative prediction.

Structural information can therefore make the abundance correlations interpretable, but what they reveal need not be niche overlap. With resource-mediated forcing, correlations can instead report the internal yield-depletion organization that was eliminated in passing to the Lotka-Volterra description. Thus, the same effective interaction matrix can be associated with positive, vanishing, or negative equal-time correlations, depending on mechanistic information that $\boldsymbol{\alpha}$ itself does not contain.

V. DISCUSSION

The central result of this paper is an identifiability limit. Equal-time abundance correlations are determined jointly by

ecological interactions and by the structure of environmental forcing, and therefore do not identify the interaction matrix without additional mechanistic information. A natural benchmark is obtained when similarity in environmental response matches competitive similarity, $C^{(\eta)} = \boldsymbol{\alpha}_S$. At this matched point, the two effects cancel exactly and all equal-time interspecific correlations vanish. Away from it, nonzero correlations are generated by the response-competition mismatch, while the interaction matrix controls how that mismatch is propagated through the community.

Standard ecological descriptions often integrate out the resource dynamics and retain only an effective interaction matrix, interpreted here as niche overlap. To the extent that this coarse-grained description is adequate, the resource timescales and the separate yield and depletion structures are dynamically irrelevant and provide no independent biological reference against which the response-competition mismatch can be judged. A mechanistic benchmark for the mismatch appears only when degrees of freedom eliminated by the coarse graining become dynamically relevant. Keeping those degrees of freedom exposes two such benchmarks, one temporal and one structural.

The two benchmarks lead to qualitatively different interpretations of the correlation signal. A temporal mismatch arises when the shared environmental response is effectively immediate while competition is transmitted through resources on a finite timescale. In this case, the cancellation is broken and the correlations can track niche overlap. A structural mismatch arises when the environment itself acts through the resources: The forcing inherited by the consumers then depends on $\Gamma\Gamma^T$, whereas competition depends on $\Gamma\Lambda$. The correlations consequently reflect the relation between yield and depletion rather than niche overlap alone. In both cases, the interpretation of equal-time correlations depends on mechanistic information that is not contained in the correlation matrix itself.

A. Relation to dynamical inference methods

Throughout this paper, we consider only equal-time abundance correlations. It is the most accessible of the fluctuation statistics: It requires only that abundances be recorded, and being an average it is comparatively robust to measurement error. Two other families of inference read more from the same fluctuations, and it is worth placing our result beside them.

The first estimates the interaction matrix from the rate of change of the abundances, fitting the growth rate to the abundance, or equivalently, taking a short-lag derivative of the covariance [30–33]. In the white-noise limit, this is exact: Writing $\Sigma(\tau) = \langle \delta n(t+\tau)\, \delta n(t)^T \rangle = e^{J\tau}\Sigma(0)$ for $\tau > 0$, the one-sided derivative at $\tau = 0^+$ gives the drift $J = -N\boldsymbol{\alpha}$. Therefore, $J = \dot{\Sigma}(0)\,\Sigma(0)^{-1}$. The degeneracy we have described is broken because the derivative supplies the second moment $\langle \dot{n}\, n \rangle$ that the correlation alone omits.

But the exactness is fragile, in three independent ways. When the environmental forcing carries temporal structure, as ecological forcing generally does, the cross term $\langle \eta\, n \rangle$ no longer vanishes and the estimate is biased. Because it rests on a numerical derivative, it amplifies measurement error, inflating the high-frequency content where noise dominates. Even with white noise and perfect data, the derivative must be taken at a finite sampling interval, adequate only for modes whose relaxation time it resolves: A real community carries a *spread* of relaxation timescales, and a single finite sampling interval may fail to resolve them unless the temporal resolution and the record length together span the full dynamical range. What is a virtue of the equal-time correlation, that it is a stationary quantity, integrating over time rather than differentiating, and indifferent to the sampling rate, is precisely what these methods give up.

A second family, developed by Chen *et al.* [4], reads the fluctuations not through the equal-time correlation but through their full frequency content, using the cross-spectrum and the coherence. This is a genuinely different probe, aimed at a different target: Not the interaction matrix $\boldsymbol{\alpha} = \Gamma\Lambda$, but the structure of shared resource use $\Gamma\Gamma^T$, which guild a species belongs to, rather than how strongly it competes. In our decomposition, that target is the response channel, the very object the correlations do carry, and the two coincide under the proportional yield-depletion benchmark. Their method relies on the environment being temporally structured, the coherence between two species is the signature of their common, colored, resource-mediated drive.

The three approaches are therefore complementary rather than competing: They read different moments of the same fluctuations, and they are sensitive to different aspects of the dynamics: the response-competition mismatch, the interactions under white forcing, and the resource-sharing structure, respectively. But all three differ only in *which* statistic they read. A different question is when equal-time correlations themselves can become informative once independent information about the ordering of species pairs is supplied.

B. Mechanistic interpretation with external information

Equal-time abundance correlations do not, by themselves, identify the mechanism that produced them. They can become mechanistically informative, however, when combined with independent information about the ecological organization of species pairs. A particularly useful example is an external proxy for niche overlap, such as phylogenetic or genetic relatedness. Such information does not add another fluctuation statistic; rather, it supplies an independent ordering of species pairs against which the observed correlation pattern can be compared. This makes it possible to ask not only whether species fluctuate together, but whether the way they do so is consistent with temporal mismatch, structural mismatch, or neither.

Suppose, for example, that phylogenetic or genetic relatedness provides a proxy for niche overlap, so that α_{ij} tends to decrease with the distance between species i and j. If the measured correlations ρ_{ij} decrease with that distance, as reported by Sireci *et al.* [2], then the community cannot be described by the instantaneous matched limit, in which all equal-time interspecific correlations vanish. Within the mechanisms considered here, such an ordering is naturally produced when environmental forcing acts directly on the consumers while competitive feedback is delayed by the resource dynamics: Increasing niche overlap then strengthens the positive correlation exposed by the delay. Resource-mediated forcing, in

contrast, need not preserve this ordering because the correlation also depends on the separate yield and depletion structures. Thus, given an independent ordering by niche overlap, the observed trend can support a temporal-mismatch interpretation, although it does not identify that mechanism uniquely.

A different situation arises when the route of environmental forcing is known independently. Suppose, for example, that environmental variability enters primarily through the resources, as in a chemostat with fluctuating nutrient supply. The relevant comparison is then not between the abundance correlation and niche overlap alone, but between the covariance inherited through the resources, $\Gamma\Gamma^T$, and the competitive structure $\Gamma\Lambda$. Under the globally proportional benchmark $\Lambda = c\,\Gamma^T$, these structures are matched and the equal-time interspecific correlations vanish. Nonzero correlations therefore indicate a departure from this matched resource-mediated benchmark. More generally, their sign and magnitude carry information about the structural mismatch between yield and depletion, although they do not provide a direct or unique measure of that mismatch.

A vanishing correlation is less diagnostic. Both of the matched benchmarks considered here predict zero equal-time interspecific correlations: direct consumer forcing with effectively instantaneous competitive feedback, and resource-mediated forcing with matched yield and depletion structures. Other parameter combinations may also produce cancellations, so observing $\rho_{ij} = 0$ does not identify either mechanism. If the route of environmental forcing or the relevant timescale is known independently, however, a null result can still constrain the possible mismatch and test whether the corresponding matched benchmark is approximately satisfied.

If an independent proxy for niche overlap is also available, the pattern of scatter at fixed overlap provides an additional diagnostic. Under delayed competitive feedback with direct consumer forcing, species pairs with similar α_{ij} are expected to have similar correlations, and in the simple regime studied here the points approximately collapse onto a single increasing relation between ρ_{ij} and α_{ij}. Under resource-mediated forcing, this collapse is generally lost because pairs with the same effective overlap can differ in their underlying yield and depletion structures. The same value of α_{ij} may then be associated with correlations of different magnitudes, or even opposite signs. Such sign variation at fixed overlap is therefore a possible signature of structural mismatch, although, like the mean trend itself, it is not by itself a unique identification of the underlying mechanism.

Taken together, these examples illustrate the limited but potentially useful role of equal-time abundance correlations. By themselves they do not identify niche overlap, the route of environmental forcing, or the underlying resource-use structure. When combined with independent information about one of these elements, however, they can constrain the others and help discriminate among mechanistic interpretations. Their value therefore lies not in providing a direct map of ecological interactions, but in becoming informative once the otherwise underdetermined inference problem is supplemented by external biological information.

ACKNOWLEDGMENTS

N.M.S. acknowledges support from the Israel Ministry of Innovation, Science and Technology (Italy-Israel cooperation, Grant No. 7578) and from the Israel Science Foundation (Grant No. 2435/24).

DATA AVAILABILITY

There are no publicly available research data or software supporting this manuscript. Requests for further information or data should be sent to the authors.

APPENDIX A: GENERATING Γ AND Λ

Everything in Secs. IV A and IV B rests on being able to produce many pairs (Γ, Λ) that yield the *same* niche-overlap matrix $\boldsymbol{\alpha} = \Gamma\Lambda$ while differing in the yield-depletion relation. This Appendix specifies how that is done.

We adopted an approach in which both matrices were determined together, by constrained optimization, and the non-negativity is imposed as a bound rather than checked afterward.

Given a target interaction matrix $\boldsymbol{\alpha}$, with $\alpha_{ii} = 1$ and a prescribed mean overlap, we minimize

$$\mathcal{C}(\Gamma, \Lambda) = \frac{\| \Gamma\Lambda - \boldsymbol{\alpha} \|_F^2}{\| \boldsymbol{\alpha} \|_F^2} + w \sum_{i=1}^{S} \left(\sum_{k=1}^{Q} \gamma_{ik} - 2 \right)^2, \qquad 0 \leqslant \gamma_{ik}, \quad \lambda_{ki} \leqslant 2 \tag{A1}$$

by sequential quadratic programming, from a starting point drawn uniformly on [1, 2]. We take $w = 0.1$.

The first term asks that the pair reproduce the required niche overlap. The second enforces the normalization of Sec. II: Rows of Γ summing to 2 give $r_i = \sum_k \gamma_{ik} - 1 = 1$, so that all species share the same intrinsic growth rate.

Different random starting points converge to different (Γ, Λ) that reproduce the *same* $\boldsymbol{\alpha}$. This is the degeneracy the paper is about, and it is what supplies the spread of yield-depletion mismatch at fixed niche overlap in Figs. 3 and 4.

1. What the procedure delivers

Because Eq. (A1) is minimized rather than solved, the two requirements compete, and neither is met exactly. Both must therefore be reported rather than assumed. Table I gives them, over 40 independent runs for each parameter set.

2. Rejection criteria

A pair (Γ, Λ) that reproduces $\boldsymbol{\alpha}$ need not describe a viable community. We discard it unless

(1) $\lambda_{ki} \geqslant 0$ for all k, i (guaranteed by the box constraints),
(2) the coexistence fixed point is positive, $\bar{n}_i > 0$ for all i,
(3) the quasisteady resource abundances are positive, $\bar{R}_k = 1 - \sum_i \lambda_{ki}\bar{n}_i > 0$ for all k,
(4) that fixed point is linearly stable.

Acceptance is high: 40/40 for $S = 2$, $Q = 3$ at mean overlap 0.4 and 0.6, 39/40 at 0.8, and 40/40 for $S = 5$, $Q = 8$ at mean overlap 0.3. The rejections occur at strong overlap, where $\bar{R}_k$ approaches zero.

TABLE I. Accuracy of the sampler, median over 40 runs. The worst case over all runs and all parameter sets is 2×10^{-6} in each column. The reconstructed interaction matrix agrees with the target, the rows of Γ sum to 2 so that $r_i = 1$, and the diagonal of $\Gamma\Lambda$ is unity, all to within numerical tolerance. The residual is small enough that the intrinsic growth rates may be treated as uniform for the purposes of the calculations below.

S	Q	α	$\frac{\|\Gamma\Lambda-\boldsymbol{\alpha}\|_F}{\|\boldsymbol{\alpha}\|_F}$	$\max_i \lvert\sum_k \gamma_{ik} - 2\rvert$	diag($\Gamma\Lambda$)
2	3	0.6	1.4×10^{-7}	1.7×10^{-7}	1.0000
2	3	0.4	1.2×10^{-7}	3.5×10^{-7}	1.0000
2	3	0.8	1.2×10^{-7}	2.5×10^{-7}	1.0000
5	8	0.3	5.5×10^{-7}	4.7×10^{-7}	1.0000

APPENDIX B: DERIVATION OF THE REDUCED LYAPUNOV EQUATION

This Appendix derives Eq. (15), on which the whole of Sec. III rests, and establishes the uniqueness of its solution. No symmetry of $\boldsymbol{\alpha}$ is assumed at any point.

1. The reduction

We start from the Lyapunov equation (11) with the drift and diffusion matrices of Eqs. (9) and (10),

$$J\,\Sigma + \Sigma\,J^T + D = 0, \quad J = -N\boldsymbol{\alpha}, \quad D = \sigma_e^2\,N\,C^{(\eta)}N, \tag{B1}$$

and substitute the ansatz

$$\Sigma = \frac{\sigma_e^2}{2}\,N + N\,Y\,N, \tag{B2}$$

with Y symmetric. Expanding

$$\begin{aligned} J\Sigma + \Sigma J^T + D &= -N\boldsymbol{\alpha}\left(\frac{\sigma_e^2}{2}N + NYN\right) \\ &\quad - \left(\frac{\sigma_e^2}{2}N + NYN\right)\boldsymbol{\alpha}^T N + \sigma_e^2 NC^{(\eta)}N \\ &= -\frac{\sigma_e^2}{2}\,N\boldsymbol{\alpha}N - N\boldsymbol{\alpha}NYN - \frac{\sigma_e^2}{2}\,N\boldsymbol{\alpha}^T N \\ &\quad - NYN\boldsymbol{\alpha}^T N + \sigma_e^2\,NC^{(\eta)}N. \end{aligned} \tag{B3}$$

Every term carries a factor N on the left and a factor N on the right. Since N is diagonal with strictly positive entries at a coexistence fixed point, it is invertible, and we may multiply through by N^{-1} from both sides. Setting the result to zero and rearranging

$$\boldsymbol{\alpha}N\,Y + Y\,N\boldsymbol{\alpha}^T = \sigma_e^2\big(C^{(\eta)} - \tfrac{1}{2}(\boldsymbol{\alpha} + \boldsymbol{\alpha}^T)\big) = \sigma_e^2\,\boldsymbol{\beta}, \tag{B4}$$

which is Eq. (15).

Two features of this calculation are worth isolating.

(1) The symmetrization is forced, not chosen. The combination $\boldsymbol{\alpha}_S = \frac{1}{2}(\boldsymbol{\alpha} + \boldsymbol{\alpha}^T)$ arises from a single source: The first term of the ansatz, $\frac{\sigma_e^2}{2}N$, contributes $-\frac{\sigma_e^2}{2}(\boldsymbol{\alpha} + \boldsymbol{\alpha}^T)$ after the factors of N are stripped, because the Lyapunov equation contains both $J\Sigma$ and its transpose. It appears nowhere else. The symmetric part of the interaction matrix is therefore not an assumption imposed for convenience, and not a definition of niche overlap adopted in advance: It is the only part of $\boldsymbol{\alpha}$ that the equation permits a noise covariance to be compared with. A covariance matrix is symmetric, and the antisymmetric part of $\boldsymbol{\alpha}$ has nothing symmetric to be measured against.

(2) The interaction matrix is not a source. In Eq. (B4), the matrix $\boldsymbol{\alpha}$ appears twice on the left, acting on Y, and once on the right, inside $\boldsymbol{\beta}$. Its appearance on the left is that of an operator: It determines how a given source is transmitted through the community. Its appearance on the right is only as the reference against which the noise is measured. There is no term in which $\boldsymbol{\alpha}$ drives the correlations by itself.

2. Existence and uniqueness

Write $K = \boldsymbol{\alpha}N$, so that Eq. (B4) reads

$$K\,Y + Y\,K^T = \sigma_e^2\,\boldsymbol{\beta}. \tag{B5}$$

This is a Sylvester equation. The linearization presupposes a stable coexistence fixed point, and stability places every eigenvalue of $J = -N\boldsymbol{\alpha}$ in the left half plane, so every eigenvalue of $K = \boldsymbol{\alpha}N$, which shares the spectrum of $N\boldsymbol{\alpha}$, has positive real part. No two can then sum to zero, and the solution is therefore unique for any $\boldsymbol{\beta}$, symmetric or not. If $\boldsymbol{\beta} = 0$ then $Y = 0$ is that unique solution, so by Eq. (B2) the abundance covariance is $\Sigma = \frac{\sigma_e^2}{2}N$, diagonal, and every interspecific correlation vanishes identically. The cancellation therefore holds around any stable fixed point, whatever the asymmetry of $\boldsymbol{\alpha}$. Asymmetry bears only on whether the matched noise $C^{(\eta)} = \boldsymbol{\alpha}_S$ is itself admissible, which requires $\boldsymbol{\alpha}_S$ to be positive semidefinite (Appendix C 5).

3. Why the heterogeneity of α does not propagate

Decompose the interaction matrix into a homogeneous part and a perturbation, $\boldsymbol{\alpha} = \bar{\boldsymbol{\alpha}} + \delta\boldsymbol{\alpha}$, with $\bar{\boldsymbol{\alpha}}$ having unit diagonal and all off-diagonal entries equal to the mean overlap μ. The fixed point shifts with it,

$$\bar{\mathbf{n}} = \boldsymbol{\alpha}^{-1}\mathbf{1} = \bar{\boldsymbol{\alpha}}^{-1}\mathbf{1} - \bar{\boldsymbol{\alpha}}^{-1}\,\delta\boldsymbol{\alpha}\,\bar{\boldsymbol{\alpha}}^{-1}\mathbf{1} + O(\delta\boldsymbol{\alpha}^2), \tag{B6}$$

so that $N = \bar{N} + \delta N$, with $\delta N = O(\delta\boldsymbol{\alpha})$.

Now observe that the source term of Eq. (B5) is $O(\boldsymbol{\beta})$, and hence so is Y. Both $\delta\boldsymbol{\alpha}$ and δN enter the equation only through the operator on the left, that is, only multiplied by Y. Their contribution is therefore $O(\delta\boldsymbol{\alpha}\,\boldsymbol{\beta})$, and to leading order in the mismatch

$$\bar{K}\,Y + Y\,\bar{K}^T = \sigma_e^2\,\boldsymbol{\beta}, \quad \bar{K} = \bar{\boldsymbol{\alpha}}\,\bar{N}, \tag{B7}$$

in which the propagator is built from the *homogeneous* interaction matrix alone. The pairwise heterogeneity of the niche overlaps, which is the quantity the inference is trying to recover, is absent from the leading-order answer. It reappears at second order, and there it does not act as a source but as a contamination: It transmits the mismatch of one pair to the correlation of another along indirect paths $i \to k \to j$.

4. Confirmation by direct simulation

Equation (B4) is exact within the linearized weak-noise description. Since the underlying dynamics [Eq. (7)] is nonlinear and the noise multiplicative, we confirmed it against direct Stratonovich simulation of the full stochastic process

for two species. The estimated correlations converge to the values predicted by Eq. (18). In fact, at the matched point the cancellation is exact and nonperturbative in the noise strength, as we prove in Appendix C.

APPENDIX C: EXACT FACTORIZATION AT THE MATCHED POINT

The cancellation of interspecific correlations at the matched point $C^{(\eta)} = \boldsymbol{\alpha}_S$ [Eq. (13)] was obtained above from the linearized Lyapunov equation, that is, to leading order in the noise strength. At the matched point, the result is in fact exact and nonperturbative: The full nonlinear stationary distribution factorizes into independent single-species Gamma laws, for any noise strength and for arbitrary, possibly nonreciprocal, interactions. We give the derivation here.

In what follows, we use the general stochastic Lotka-Volterra system, with heterogeneous growth rates r_i and an arbitrary interaction matrix $\boldsymbol{\alpha}$,

$$dn_i = n_i\left(r_i - \sum_j \alpha_{ij}\, n_j\right) dt + \sigma_e\, n_i \circ \sum_a B_{ia}\, dW_a,$$
$$C^{(\eta)} = BB^T, \tag{C1}$$

in the Stratonovich convention (denoted by $\circ$), and assume a positive coexistence fixed point, $\bar{\mathbf{n}} = \boldsymbol{\alpha}^{-1}\mathbf{r} > 0$, so that

$$\mathbf{r} = \boldsymbol{\alpha}\,\bar{\mathbf{n}}. \tag{C2}$$

Equation (7) is the special case $r_i = 1$. We develop the argument for the standard bilinear interaction $\alpha_{ij}n_j$ and a common noise amplitude. A more general interaction term and a species-dependent amplitude, are treated at the end of the Appendix.

In the logarithmic variables $x_i = \log n_i$, the Stratonovich chain rule holds without a drift correction, and the multiplicative noise becomes additive with a constant coefficient,

$$d\mathbf{x} = -\boldsymbol{\alpha}\,\nabla U(\mathbf{x})\, dt + \sigma_e\, B\, d\mathbf{W},$$
$$U(\mathbf{x}) = \sum_i (e^{x_i} - \bar{n}_i\, x_i), \tag{C3}$$

with constant diffusion $D = \frac{1}{2}\sigma_e^2\, C^{(\eta)}$. Importantly, the potential U is *separable*, a sum of single-species terms, because the logistic nonlinearity e^{x_i} is diagonal in the site basis, and the interaction $\boldsymbol{\alpha}$ enters only as a constant mobility, not through U.

1. Symmetric interactions

Take $\boldsymbol{\alpha} = \boldsymbol{\alpha}_S$ and the matched noise $C^{(\eta)} = \boldsymbol{\alpha}_S$, so that $D = \frac{\sigma_e^2}{2}\boldsymbol{\alpha}_S$. Mobility and diffusion then satisfy an Einstein relation, $D \propto \boldsymbol{\alpha}$, and the Boltzmann distribution

$$p_*(\mathbf{x}) \propto \exp\left[-\frac{2}{\sigma_e^2}\, U(\mathbf{x})\right] \tag{C4}$$

is stationary: With $\nabla p_* = -\frac{2}{\sigma_e^2}(\nabla U)\, p_*$, the probability current

$$\mathbf{j} = -\boldsymbol{\alpha}(\nabla U)\, p_* - D\,\nabla p_* = (C^{(\eta)} - \boldsymbol{\alpha}_S)\,\nabla U\, p_* \tag{C5}$$

vanishes identically. More generally, for an arbitrary noise covariance the current is $\mathbf{j} = (C^{(\eta)} - \boldsymbol{\alpha})(\nabla U)\, p_*$. The symmetric part $C^{(\eta)} - \boldsymbol{\alpha}_S$ vanishes at the matched point, while an antisymmetric contribution $-\boldsymbol{\alpha}_A$ remains when the interactions are nonreciprocal. This case is considered below.

Because U is separable, p_* factorizes, and in the original variables

$$p_*(\mathbf{n}) = \prod_i \mathrm{Gamma}\left(\frac{2\bar{n}_i}{\sigma_e^2}, \frac{\sigma_e^2}{2}\right), \tag{C6}$$

so each species is an independent Gamma variable with $\langle n_i\rangle = \bar{n}_i$ and $\mathrm{Var}(n_i) = \frac{\sigma_e^2}{2}\bar{n}_i$. Independence gives $\langle n_i n_j\rangle = \langle n_i\rangle\langle n_j\rangle$ and hence

$$\mathrm{Cov}(n_i, n_j) = 0 \quad \text{for every } i \neq j, \tag{C7}$$

exactly and for arbitrary σ_e.

The factorization is in fact stronger than the vanishing of the covariance, since all mixed cumulants and the equal-time mutual information vanish as well. The matched noise exists provided $\boldsymbol{\alpha}_S \succeq 0$ (the symbol $\succeq$ stands for positive semidefinite), which holds automatically for a symmetric $\boldsymbol{\alpha}$ with a stable positive fixed point.

A factorized Gamma stationary distribution under a detailed-balance relation between the interaction and environmental-noise matrices was previously derived by Camacho-Mateu *et al.* [12]. In what follows, we extend the factorized solution to nonreciprocal interactions, for which the stationary state may support a nonzero but divergence free probability current.

2. Nonreciprocal interactions

Now, let $\boldsymbol{\alpha} = \boldsymbol{\alpha}_S + \boldsymbol{\alpha}_A$, with $\boldsymbol{\alpha}_A \neq 0$. Provided that $\boldsymbol{\alpha}_S$ is positive definite and that the corresponding coexistence state is feasible, $\boldsymbol{\alpha}_S$ can still define a correlation matrix, so one may choose $C^{(\eta)} = \boldsymbol{\alpha}_S$. Although the covariance can match only $\boldsymbol{\alpha}_S$, the *same* p_* of Eq. (C4) remains the stationary probability distribution function.

The only difference is that, once the interaction matrix is asymmetric, Eq. (C4) no longer satisfies detailed balance. Instead, it now carries a nonzero current,

$$\mathbf{j} = -\,\boldsymbol{\alpha}_A\,(\nabla U)\, p_*. \tag{C8}$$

This is the $\boldsymbol{\alpha}_A$ term identified in the general decomposition above: The symmetric part of the current vanishes because $C^{(\eta)} = \boldsymbol{\alpha}_S$, leaving only the antisymmetric residual.

Despite carrying a current, the probability distribution (C4) is still time independent, because this current is divergence-free. Writing $j_i = -\sum_k (\alpha_A)_{ik}\,(\partial_k U)\, p_*$,

$$\nabla\cdot\mathbf{j} = -\,p_*\sum_{i,k}(\alpha_A)_{ik}\,\partial_i\partial_k U + \frac{2}{\sigma_e^2}\,p_*\,(\nabla U)^T\boldsymbol{\alpha}_A(\nabla U)$$
$$= 0. \tag{C9}$$

Both terms in this equation vanish by the antisymmetry of $\boldsymbol{\alpha}_A$ alone: the first is the contraction of the antisymmetric $\boldsymbol{\alpha}_A$ with the symmetric Hessian $\partial_i\partial_k U$, the second the quadratic form $(\nabla U)^T\boldsymbol{\alpha}_A(\nabla U)$. Neither step uses the separability of U, so the stationarity of p_* holds for any potential. Hence, p_* remains

stationary, and the factorization (C6), with $\mathrm{Cov}(n_i, n_j) = 0$, holds verbatim for the full, nonreciprocal $\boldsymbol{\alpha}$.

As mentioned, detailed balance is now broken: The steady state supports a persistent rotational probability current and is irreversible. The interaction is thus invisible to the equal-time distribution while remaining fully present in the dynamics, in lagged correlations and in the entropy production of the abundance process. Separability enters only in the last step of the symmetric case, in reading off the factorized form. The stationarity of p_* does not require it.

3. Generalizations

(1) *General interaction.* The bilinear form $\alpha_{ij}n_j$ may be replaced by $\alpha_{ij}\,\psi_j(n_j)$ with an arbitrary species-specific monotone ψ_j, one per species [a Holling saturation $\psi_i(n) = n/(1 + k_i n)$ is one example]. Each ψ_j is absorbed into a separate coordinate V_j of the potential $U = \sum_i V_i(x_i)$, which stays separable, so the factorization persists, now with non-Gamma marginals set by ψ_i. The derivation uses only that the nonlinearity be *elementwise*: Species j acts through a function of n_j alone. An aggregate nonlinearity, $g(\sum_j \alpha_{ij}n_j)$, generally destroys separability. Whether its stationary law remains approximately factorized is a separate question.

(2) *General noise.* The matched noise of Eq. (13) has a unit diagonal, which presumes a common forcing amplitude across species. What if different species suffer from noises of different amplitude, i.e., when the covariance matrix is not unit diagonal?

Let us consider the case in which the diagonal terms of the covariance matrix of the noise are $H = \mathrm{diag}(h_1, \ldots, h_S)$, instead of $H = \sigma_e^2\mathbb{1}$. We would like to show that here also one can find a noise covariance matrix that supports a separable stationary distribution function; hence, all zero-time interspecific correlations vanish.

To achieve that, we choose a noise covariance

$$Z = \tfrac{1}{2}(\alpha H + H\alpha^T), \tag{C10}$$

which is symmetric by construction. Note that the drift in log variables $d\mathbf{x} = -\boldsymbol{\alpha}\,(\mathbf{n} - \bar{\mathbf{n}})\,dt + \cdots$ is unchanged: It is determined by the interaction matrix $\boldsymbol{\alpha}$ and the fixed point $\bar{\mathbf{n}}$, and does not depend on H.

We then define

$$U(\mathbf{x}) = 2\sum_i \frac{e^{x_i} - \bar{n}_i x_i}{h_i}. \tag{C11}$$

Hence,

$$\nabla U = 2H^{-1}(\mathbf{n} - \bar{\mathbf{n}}). \tag{C12}$$

Substituting these expressions into the probability-current equation,

$$\mathbf{j} = \left[-\alpha(\mathbf{n} - \bar{\mathbf{n}}) + \tfrac{1}{2}Z\nabla U\right]e^{-U}, \tag{C13}$$

we obtain

$$\mathbf{j} = -\tfrac{1}{2}(\alpha H - H\alpha^T)H^{-1}(\mathbf{n} - \bar{\mathbf{n}})\,e^{-U}, \tag{C14}$$

which is divergence-free,

$$\nabla \cdot \mathbf{j} = 0. \tag{C15}$$

The construction so far only requires Z to be symmetric. For it to be a genuine noise covariance, one also needs admissibility, the existence of a real B with $\sigma_e^2 BB^T = Z$. This is more restrictive than $\boldsymbol{\alpha}_S \succeq 0$: It requires the H-weighted symmetric part $S_H = \frac{1}{2}(H^{-1/2}\boldsymbol{\alpha}H^{1/2} + H^{1/2}\boldsymbol{\alpha}^T H^{-1/2}) \succeq 0$. However, when this condition is satisfied, once again the stationary probability density factorizes into a product of Gamma distributions:

$$P_{\mathrm{st}}(\mathbf{n}) = \prod_i \frac{1}{\Gamma(2\bar{n}_i/h_i)}\left(\frac{2}{h_i}\right)^{2\bar{n}_i/h_i} n_i^{2\bar{n}_i/h_i - 1}\exp\left(-\frac{2n_i}{h_i}\right). \tag{C16}$$

Equivalently,

$$n_i \sim \mathrm{Gamma}\left(\frac{2\bar{n}_i}{h_i}, \frac{h_i}{2}\right), \tag{C17}$$

where the second argument is the scale parameter.

This case, different levels of stochasticity for different species, manifests itself when the forcing is resource mediated, as in Sec. IV B. $C^{\mathrm{eff}} = \sigma_r^2\Gamma\Gamma^T$ has a nonuniform diagonal, $H = \mathrm{diag}(C^{\mathrm{eff}})$, and its exact-cancellation condition is Eq. (C10).

(3) *Itô convention.* The derivation is in the Stratonovich convention, natural if the white noise is the short-correlation limit of an external forcing. In the Itô convention, the same factorization survives, with the Gamma means shifted by the usual noise-induced drift, $\bar{\mathbf{n}} \mapsto \boldsymbol{\alpha}^{-1}(\mathbf{r} - \frac{1}{2}\,\mathrm{diag}\,Z)$. The difference is a shift of the coexistence point, not a change in the result. This shift is the multispecies counterpart of the mean $\bar{n}_i = K_i(1 - \sigma_i^2/2)$ of the single-species logistic model with carrying capacity K.

4. The Gamma distribution

The product-form stationary distribution is thus an alternative route to the Gamma abundance laws familiar from neutral models and from noninteracting stochastic-logistic models [5,34]: There the independent Gamma marginals arise because the species do not interact, or interact only through a mean field, whereas here they arise for an arbitrary interaction matrix, provided the environmental noise is matched to it. The Gamma abundance distributions and the vanishing equal-time correlations are all properties of the noise structure, not of the interactions. The independence of the equal-time marginals, in particular, is not a signature of the absence of interactions. It is a signature of the fluctuation-dissipation balance $C^{(\eta)} = \boldsymbol{\alpha}_S$ between the noise and the competition. The interactions are not absent; they are hidden: Present in the dynamics, in the lagged correlations, and, for nonreciprocal $\boldsymbol{\alpha}$, in the entropy production of the irreversible steady state, yet invisible to the equal-time distribution. One may conjecture that in the close neighborhood of the matched point the single-species abundances remain approximately Gamma distributed while the interspecific correlations already turn on, positive or negative according to the sign of the mismatch β, so that standard single-species distributions and nontrivial pairwise correlations coexist, as observed empirically and reproduced by the interaction-based model of Camacho-Mateu *et al.* [5].

5. Admissibility of the matched noise

Throughout this paper, we assume that the noise covariance prescribed at the matched point is admissible, namely, that it is symmetric and positive semidefinite and can therefore be realized as the covariance of a multivariate noise process. We now make this condition explicit.

Consider first the normalization $C^{(\eta)}_{ii} = \alpha_{ii} = 1$. The matched noise correlation matrix is then

$$C^{(\eta)} = \boldsymbol{\alpha}_S, \quad \boldsymbol{\alpha}_S \equiv \tfrac{1}{2}(\boldsymbol{\alpha} + \boldsymbol{\alpha}^T). \tag{C18}$$

Consequently, the matched noise is admissible if and only if $\boldsymbol{\alpha}_S \succeq 0$.

For symmetric interactions, admissibility follows automatically from stable coexistence. Let $N = \mathrm{diag}(\bar{n}_1, \ldots, \bar{n}_S) \succ 0$, where the symbol $\succ$ implies positive definite, so that the Jacobian at the coexistence fixed point is $J = -N\boldsymbol{\alpha}$. If the fixed point is linearly stable, all eigenvalues of $N\boldsymbol{\alpha}$ are positive. Since $\boldsymbol{\alpha}$ is symmetric, $N\boldsymbol{\alpha}$ is similar to the symmetric matrix

$$N^{-1/2}(N\boldsymbol{\alpha})N^{1/2} = N^{1/2}\boldsymbol{\alpha}N^{1/2}. \tag{C19}$$

The latter therefore has only positive eigenvalues and is positive definite. Moreover, $N^{1/2}\boldsymbol{\alpha}N^{1/2}$ is related to $\boldsymbol{\alpha}$ by a congruence transformation. Sylvester's law of inertia implies that a transformation of this type keeps the number of positive, negative, and zero eigenvalues, therefore $\boldsymbol{\alpha} \succ 0$. Thus, conditional on feasibility, stable coexistence for a symmetric interaction matrix implies that $C^{(\eta)} \succ 0$, and the matched noise is admissible. Conversely, $\boldsymbol{\alpha} \succ 0$ implies stability of the positive fixed point. Hence, for symmetric interactions and conditional on feasibility,

$$\text{stability} \iff \boldsymbol{\alpha} \succ 0 \iff C^{(\eta)} = \boldsymbol{\alpha} \text{ is admissible.} \tag{C20}$$

For asymmetric interactions, this implication no longer holds. Stability of $J = -N\boldsymbol{\alpha}$ does not, in general, imply $\boldsymbol{\alpha}_S \succeq 0$. With common forcing amplitudes, admissibility of the matched noise therefore requires the additional condition $\boldsymbol{\alpha}_S \succeq 0$. A sufficient condition is that the symmetric interaction matrix $\boldsymbol{\alpha}_S$, considered as a dynamical system in its own right, admit a stable positive fixed point.

More generally, let $H = \mathrm{diag}(h_1, \ldots, h_S) \succ 0$ describe species-dependent forcing amplitudes. The covariance required at the matched point is

$$Z = \tfrac{1}{2}(\boldsymbol{\alpha}H + H\boldsymbol{\alpha}^T). \tag{C21}$$

This construction defines a legitimate noise covariance only when $Z \succeq 0$. Since H is positive diagonal, this condition is equivalently

$$S_H \equiv H^{-1/2}ZH^{-1/2} = \tfrac{1}{2}(H^{-1/2}\boldsymbol{\alpha}H^{1/2} + H^{1/2}\boldsymbol{\alpha}^T H^{-1/2}) \succeq 0. \tag{C22}$$

Thus, except in the symmetric common-amplitude case, dynamical stability and admissibility of the matched noise are distinct requirements.

APPENDIX D: NONIDENTIFIABILITY: SAMPLING AND ADMISSIBILITY

This Appendix gives the explicit construction underlying the nonidentifiability argument of Sec. III, illustrates it in Fig. 5, and tests the one condition that is not guaranteed by the Lyapunov algebra itself: Whether the environmental correlation matrix required to reproduce a given set of abundance correlations is physically admissible.

1. The construction

Let $\mathcal{R}^*$ denote a target equal-time abundance correlation matrix. Because correlations do not specify the marginal abundance variances, introduce

$$V = \mathrm{diag}(v_1, \ldots, v_S), \quad \Sigma^*(V) = V^{1/2}\mathcal{R}^*V^{1/2}, \tag{D1}$$

where $v_i > 0$ are initially free. Thus, every choice of V gives a covariance matrix with exactly the same target correlation matrix $\mathcal{R}^*$.

Now, choose any candidate interaction matrix $\boldsymbol{\alpha}$ that admits a stable positive coexistence state. The candidate fixes its own equilibrium and linearized drift,

$$\bar{\mathbf{n}} = \boldsymbol{\alpha}^{-1}\mathbf{1}, \quad N = \mathrm{diag}(\bar{n}_1, \ldots, \bar{n}_S), \quad J = -N\boldsymbol{\alpha}. \tag{D2}$$

For any chosen V, the diffusion matrix required to produce $\Sigma^*(V)$ is fixed uniquely by the Lyapunov equation,

$$D = -[J\Sigma^*(V) + \Sigma^*(V)J^T], \tag{D3}$$

and the corresponding environmental-response correlation matrix is

$$C^{(\eta)} = \sigma_e^{-2}N^{-1}DN^{-1}. \tag{D4}$$

These are precisely the operations summarized in Eq. (12). By construction, the candidate system reproduces $\Sigma^*(V)$ exactly, and therefore reproduces the prescribed correlation matrix $\mathcal{R}^*$ exactly. No fitting of the pairwise correlations is involved.

2. What must be checked

Steps (D2)–(D4) return a symmetric matrix. They do not, by themselves, guarantee a legitimate environmental correlation matrix. For $C^{(\eta)}$ to be admissible, it must be positive semidefinite, and with the normalization used in the main text it must also have unit diagonal.

The distinction between covariance and correlation data is important here. The target matrix $\mathcal{R}^*$ fixes the normalized pairwise correlations but leaves the S marginal variances v_i unspecified. We use precisely these S degrees of freedom to impose the S conditions

$$C^{(\eta)}_{ii} = 1, \quad i = 1, \ldots, S. \tag{D5}$$

We solve these conditions numerically for v_i and then test whether the resulting $C^{(\eta)}$ is positive definite. Thus, the numerical test concerns only admissibility of the forcing required by a candidate interaction matrix; the reproduction of the target abundance correlations is exact by construction.

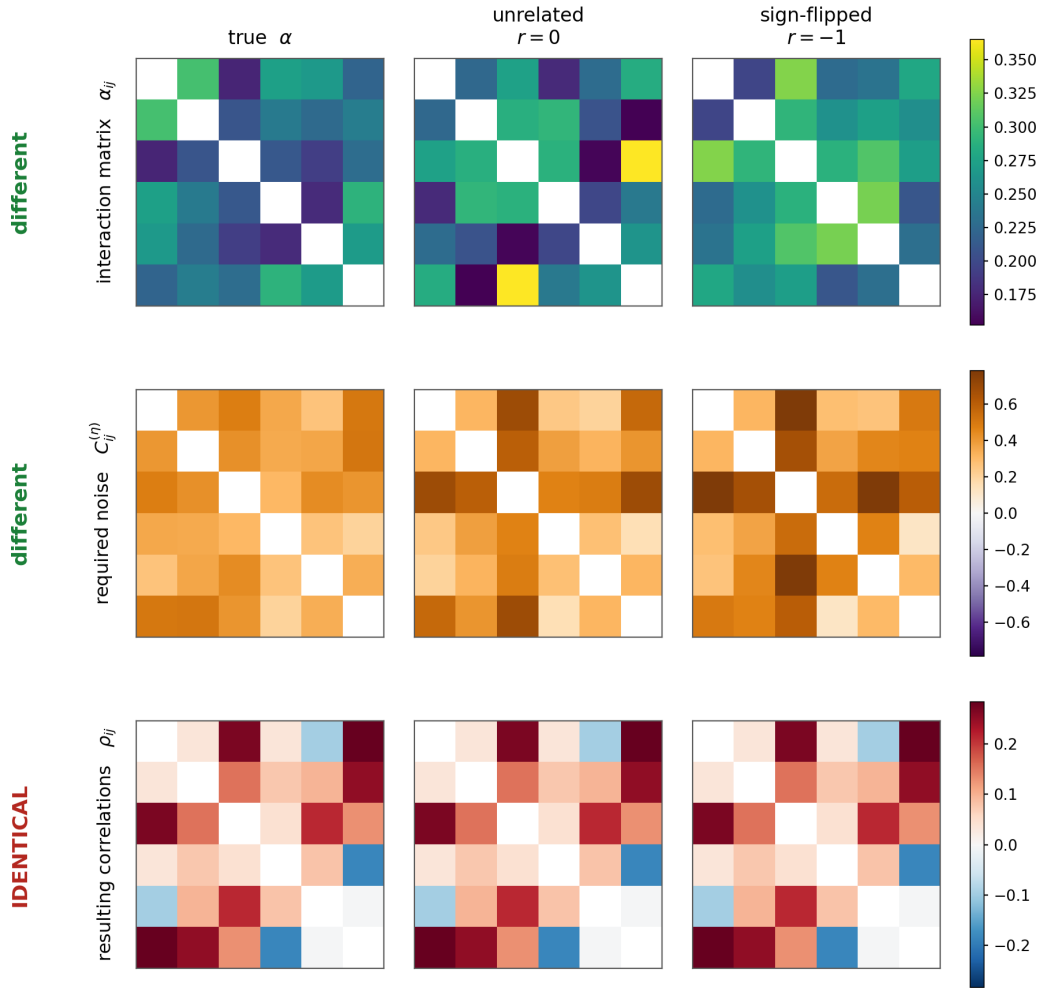


FIG. 5. The interaction matrix cannot be recovered from equal-time correlations. Three communities of $S = 6$ species with different interaction matrices are shown in the top row. All three matrices are legitimate, with positive off-diagonal entries in the range [0.15, 0.37] and a stable coexistence fixed point. The middle row shows the environmental-response correlation matrix $C^{(\eta)}$ required by each candidate, obtained from Eq. (12) after choosing the marginal abundance variances so that $C_{ii}^{(\eta)} = 1$. The bottom row shows the resulting abundance correlations, which are identical in all three cases. The interaction matrices in the left and middle columns are independent draws with the same mean overlap but no pairwise relation. In the right column, the heterogeneity is reversed relative to the left: Pairs with the strongest overlap in the true community are assigned the weakest overlap, and conversely. Thus, even the pairwise ordering of the interactions can be reversed while leaving the equal-time abundance correlation matrix unchanged.

3. Sampling

We generate the synthetic data from a "true" interaction matrix whose off-diagonal entries are

$$\alpha_{ij} = 0.25 + \delta_{ij}, \quad i \neq j, \tag{D6}$$

where $\delta_{ij} = \delta_{ji}$ are Gaussian variables with standard deviation 0.09, and $\alpha_{ii} = 1$. The environmental-noise correlation matrix is drawn independently, with

$$C_{ij}^{(\eta)} = 0.35 + w_{ij}, \quad i \neq j, \tag{D7}$$

where $w_{ij} = w_{ji}$ are Gaussian variables with standard deviation 0.10, and $C_{ii}^{(\eta)} = 1$. Draws are rejected unless both matrices are positive definite and the interaction matrix admits a positive coexistence fixed point. We take $S = 6$.

For each realization, the true interaction and noise matrices generate a target abundance correlation matrix. We then discard the true interaction matrix and ask whether the same abundance correlations can be explained by each of three deliberately incorrect candidates:

(1) an independent interaction matrix, drawn from the same ensemble and having the same mean overlap, but unrelated to the true matrix pair by pair;

(2) a permuted interaction matrix, obtained by shuffling the off-diagonal entries of the true matrix among species pairs. It therefore has exactly the same distribution of interaction strengths as the true matrix, but assigns those strengths to different pairs;

(3) a sign-flipped interaction matrix, $\alpha_{ij} \mapsto 2\mu - \alpha_{ij}$, which reverses the pairwise ordering of the interactions: The pairs with the strongest overlap in the true community are assigned the weakest overlap in the candidate, and conversely.

For each candidate, the S marginal abundance variances are chosen according to Eq. (D5). The resulting covariance matrix $\Sigma^*(V)$ may therefore have different marginal variances for different candidate interaction matrices, but its normalized

TABLE II. Very different interaction matrices generally require physically admissible environmental noise. Results for $S = 6$ over 200 independently generated communities. The second column is the mean Pearson correlation between the off-diagonal entries of the candidate and true interaction matrices. The third column counts the realizations for which the environmental-noise correlation matrix required by the candidate is positive definite. Its diagonal is fixed to unity by the choice of the marginal abundance variances. Every candidate reproduces the same target abundance correlation matrix exactly by construction; the table tests only whether the environmental forcing required to do so is itself a legitimate correlation matrix.

Candidate interaction matrix	Mean correlation with the true interactions	Reconstructed noise positive definite
Independent	+0.02	199/200
Permuted	−0.03	200/200
Sign flipped	−1.00	200/200

correlation matrix is always the same target $\mathcal{R}^*$. The only remaining question is whether the environmental correlation matrix required by the candidate is positive definite.

Figure 5 shows one representative realization of this construction. The left column is the true interaction matrix, the middle column an independently drawn candidate, and the right column a candidate in which the pairwise ordering of the true interactions is reversed. Despite their radically different interaction structures, all three reproduce the same equal-time abundance correlations when accompanied by the appropriate environmental forcing.

4. Results

Table II summarizes 200 independent realizations. For every admissible candidate, the covariance $\Sigma^*(V)$ associated with that candidate reproduces the prescribed abundance correlation matrix exactly. Substitution back into the Lyapunov equation gives maximum numerical residuals of 2×10^{-18} for the independent and permuted candidates and 3×10^{-18} for the sign-flipped candidate, confirming the algebraic construction to machine precision.

The ambiguity is not confined to candidate matrices that resemble the true interactions. An independently drawn matrix requires a positive-definite noise correlation matrix in 199 of the 200 realizations, while both the permuted and sign-flipped candidates do so in every realization. Thus, even an interaction matrix that is unrelated, or exactly anticorrelated, with the true pairwise structure can reproduce the same abundance correlations using an ordinary, physically admissible environmental-noise correlation matrix. The nonidentifiability is therefore not merely an algebraic consequence of allowing an arbitrary symmetric matrix on the right-hand side of the Lyapunov equation.

5. Behaviour with community size

Whether the degeneracy persists in larger communities must be asked at a fixed distance from the boundary of stability, rather than at fixed interaction heterogeneity. For the random interaction ensemble used here, the spectral width of the heterogeneous part grows as $2\sigma_\delta\sqrt{S}$. Thus, holding σ_δ fixed while increasing S drives the community toward the instability threshold

$$2\sigma_\delta\sqrt{S} = 1 - \mu. \tag{D8}$$

Near this threshold, a soft mode dominates the covariance and progressively restricts the set of environmental correlation matrices capable of reproducing it. The appropriate control parameter is therefore the reduced coupling,

$$g = \frac{2\sigma_\delta\sqrt{S}}{1-\mu}, \tag{D9}$$

rather than S itself.

We repeated the admissibility test of the previous subsection along lines of constant g, scaling $\sigma_\delta \propto S^{-1/2}$ so that every community sits equally far from the stability boundary, and restricting the candidates to matrices that are themselves valid stable communities. At fixed g, the admissible fraction does not fall with S: An independently drawn candidate remains admissible in essentially every realization, from a handful of species to several tens. The contraction that appears when σ_δ is instead held fixed is a near-critical effect, governed by g and setting in only as $g \to 1$. It is not a property of diversity.

The degeneracy therefore does not close as the community grows. At any S, and at any fixed distance from criticality, the interaction matrix is not determined by the correlations alone.

This complements the large-S result of Appendix E: The set of interaction matrices compatible with a given equal-time correlation pattern remains open, while the leading pairwise correlation signal is controlled by the centered response-competition mismatch rather than by the pair-to-pair variation in niche overlap.

APPENDIX E: ABUNDANCE CORRELATIONS FOR ARBITRARY S

The question addressed here is whether the environmental noise still governs the abundance correlations when the community is large, or whether its imprint is averaged away as the number of species grows. To settle it, this Appendix derives Eq. (22), defines the quantity $\tilde{\beta}_{ij}$ appearing in it, and gives the closed form valid at any community size. Throughout we work to leading order in the mismatch, using Eq. (21), in which the propagator is built from the homogeneous interaction matrix alone.

1. Solving the propagator equation

Let $\bar{\boldsymbol{\alpha}} = (1-\mu)\mathbb{1} + \mu\,\mathbf{J}$, with $\mathbf{J}$ the matrix of ones, so that $\bar{\alpha}_{ii} = 1$ and $\bar{\alpha}_{ij} = \mu$ for $i \neq j$. The fixed point is uniform,

$$\bar{n}_i = \bar{n} = \frac{1}{1+(S-1)\mu} \quad \text{for every } i, \tag{E1}$$

so $\bar{N} = \bar{n}\,\mathbb{1}$ and $\bar{K} = \bar{n}\,\bar{\boldsymbol{\alpha}}$. Equation (21) then becomes

$$\bar{\boldsymbol{\alpha}}\,Y + Y\,\bar{\boldsymbol{\alpha}} = \frac{\sigma_e^2}{\bar{n}}\,\boldsymbol{\beta} \;\equiv\; \mathbf{q} \tag{E2}$$

using the symmetry of $\bar{\boldsymbol{\alpha}}$. Substituting $\bar{\boldsymbol{\alpha}} = (1-\mu)\mathbb{1} + \mu\mathbf{J}$ and writing $y_i = \sum_k Y_{ik}$ for the row sums of Y, which is sym-

metric, we have $(\mathbf{J}Y + Y\mathbf{J})_{ij} = y_i + y_j$, and Eq. (E2) reduces to a scalar relation for each pair,

$$2(1-\mu)\,Y_{ij} + \mu\,(y_i + y_j) = q_{ij}. \tag{E3}$$

The y_i follow by summing. Writing $q_i^{\Sigma} = \sum_j q_{ij}$ and $\mathcal{Q} = \sum_{ij} q_{ij}$, and $\mathcal{Y} = \sum_k y_k$, one obtains

$$\mathcal{Y} = \frac{\mathcal{Q}}{2[1+(S-1)\mu]}, \quad y_i = \frac{q_i^{\Sigma} - \mu\,\mathcal{Y}}{2+(S-2)\mu}, \tag{E4}$$

and then Y_{ij} from Eq. (E3). The symbols y_i and $\mathcal{Y}$ are internal to this step, whereas the quantities c_i introduced below in Eq. (E7) are row means of $\boldsymbol{\beta}$ and are a different object.

2. The correlations

Since $\bar{N} = \bar{n}\,\mathbb{1}$, the ansatz (14) gives $\Sigma_{ij} = \bar{n}^2 Y_{ij}$ off the diagonal and $\Sigma_{ii} = \frac{\sigma_e^2}{2}\bar{n} + \bar{n}^2 Y_{ii}$ on it. To first order in $\boldsymbol{\beta}$, the second term of Σ_{ii} is negligible, and $\rho_{ij} \simeq (2\bar{n}/\sigma_e^2)\,Y_{ij}$. Substituting Eqs. (E3) and (E4), the factors of σ_e^2 and $\bar{n}$ cancel, and we are left with a formula in $\boldsymbol{\beta}$ alone:

$$\rho_{ij} = \frac{\beta_{ij}}{1-\mu} - \frac{\mu\,(s_i+s_j)}{(1-\mu)[2+(S-2)\mu]} + \frac{2\mu^2\,T}{(1-\mu)[1+(S-1)\mu][2+(S-2)\mu]} \tag{E5}$$

for $i \neq j$, where

$$s_i = \sum_k \beta_{ik}, \quad T = \sum_{k<l} \beta_{kl}. \tag{E6}$$

3. The large-S limit, and the definition of $\tilde{\beta}$

Equation (E5) has three terms, and they behave differently as the community grows. Introduce the row means and the grand mean of the mismatch,

$$c_i = \frac{1}{S}\sum_k \beta_{ik} = \frac{s_i}{S}, \quad m = \frac{1}{S^2}\sum_{k,l}\beta_{kl} = \frac{2T}{S^2}. \tag{E7}$$

For $S\mu \gg 1$, the denominators simplify, $2+(S-2)\mu \to S\mu$ and $1+(S-1)\mu \to S\mu$, and the second and third terms of Eq. (E5) become $(c_i + c_j)/(1-\mu)$ and $m/(1-\mu)$, respectively. Hence,

$$\rho_{ij} \longrightarrow \frac{\tilde{\beta}_{ij}}{1-\mu}, \quad \tilde{\beta}_{ij} \equiv \beta_{ij} - c_i - c_j + m, \tag{E8}$$

which is Eq. (22), and which defines $\tilde{\beta}_{ij}$: It is the mismatch of the pair (i, j) with the row, column, and overall means removed. It is the residual of a two-way decomposition of $\boldsymbol{\beta}$, and it is what remains of the mismatch once everything that can be attributed to the individual species, or to the community as a whole, has been subtracted. The correlation therefore becomes *centered* at large S, not small: Diversity removes the collective content of the mismatch, but $\tilde{\beta}_{ij}$ is an $O(1)$ quantity, so ρ_{ij} does not vanish. The noise continues to set the correlations at every community size.

Numerically, for $S = 60$, $\mu = 0.2$ and a homogeneous $\boldsymbol{\alpha}$ [so that Eq. (E5) is exact rather than leading order, the heterogeneous case of Fig. 2 gives $r = 0.98$]: The correlation between ρ_{ij} and $\tilde{\beta}_{ij}/(1-\mu)$ across the 1770 pairs is $r = 0.9998$, with slope 1.001. Against the *uncentered* $\beta_{ij}/(1-\mu)$, the agreement is visibly worse, $r = 0.990$ with slope 0.977, which is the signature of the collective terms that the centering removes.

The interpretation is the point of the exercise. Whatever part of the mismatch is shared by a species with all its competitors, or by the community as a whole, is suppressed: The first is absorbed into c_i, the second into m, and both are divided out. What survives, and what a correlation measurement returns, is the part of the mismatch that is specific to *that pair*. Increasing diversity therefore does not average the ambiguity away. It localizes it: In a large community, the correlation of a pair becomes a clean readout of that pair's own mismatch, and of nothing else. Diversity sharpens the degeneracy rather than blurring it.

APPENDIX F: MATCHED FORCING WITH DELAYED COMPETITION: DERIVATION OF EQ. (27)

This Appendix derives Eq. (27) for the stochastic consumer-resource system [Eq. (23)], with direct consumer forcing matched to the interactions [Eq. (26)] and a finite resource timescale. We assume that the interaction matrix $\boldsymbol{\alpha} = \Gamma\Lambda$ is symmetric, with $\alpha_{ii} = 1$, so that $\boldsymbol{\alpha}_S = \boldsymbol{\alpha}$, and that the resource levels at the coexistence fixed point are equal. We measure resource abundances in units of this common value, so that $\bar{R}_k = 1$ and τ_R is the resource relaxation time at the fixed point.

Setting $\sigma_r = 0$ and linearizing about $(\bar{\mathbf{n}}, \bar{\mathbf{R}})$ gives

$$\frac{d\,\delta\mathbf{n}}{dt} = N\Gamma\,\delta\mathbf{R} + \sigma_c N\boldsymbol{\xi}(t), \quad \tau_R\frac{d\,\delta\mathbf{R}}{dt} = -\,\delta\mathbf{R} - \Lambda\,\delta\mathbf{n}, \tag{F1}$$

where $N = \mathrm{diag}(\bar{n}_i)$. At the fixed point, there is no direct linear consumer-consumer term, so competitive feedback acts through the resources. Differentiating the first equation and using the second to eliminate the resource fluctuations gives

$$\tau_R\,\delta\ddot{\mathbf{n}} + \delta\dot{\mathbf{n}} + N\boldsymbol{\alpha}\,\delta\mathbf{n} = \sigma_c N(\boldsymbol{\xi} + \tau_R\dot{\boldsymbol{\xi}}). \tag{F2}$$

Finite resource relaxation has therefore converted the instantaneous competitive feedback into a second-order response.

It is useful first to diagonalize this response. Define

$$u = N^{-1/2}\delta\mathbf{n}, \quad \widetilde{K} = N^{1/2}\boldsymbol{\alpha}N^{1/2}, \quad f = N^{1/2}\boldsymbol{\xi}. \tag{F3}$$

Then, Eq. (F2) becomes $\tau_R\ddot{u} + \dot{u} + \widetilde{K}u = \sigma_c(f + \tau_R\dot{f})$. For a stable coexistence state with symmetric interactions, $\widetilde{K}$ is symmetric and positive definite. Moreover, under the matched prescription the covariance of f is exactly $\widetilde{K}\,\delta(t-t')$. Thus, the same orthogonal transformation diagonalizes both the deterministic response and the forcing covariance.

Let $\mathcal{S}\widetilde{K}\mathcal{S}^T = M$, with $M = \mathrm{diag}(\mu_a)$, and define $y = \mathcal{S}u$ and $g = \mathcal{S}f$. Each normal mode then obeys

$$\tau_R\ddot{y}_a + \dot{y}_a + \mu_a y_a = \sigma_c(g_a + \tau_R\dot{g}_a), \quad \langle g_a(t)g_b(t')\rangle = \mu_a\delta_{ab}\delta(t-t'). \tag{F4}$$

Because both the dynamics and the forcing covariance are diagonal in this basis, different stationary modes are

uncorrelated. Since $u = \mathcal{S}^T y$, it follows immediately that

$$\langle u_i u_j \rangle = \sum_a \mathcal{S}_{ai}\mathcal{S}_{aj}\langle y_a^2 \rangle. \tag{F5}$$

The remaining calculation is therefore only that of the variance of a single damped oscillator.

For one mode, Fourier transformation of Eq. (F4) gives

$$y_a(\omega) = \sigma_c \frac{1 + i\omega\tau_R}{\mu_a - \tau_R\omega^2 + i\omega}\, g_a(\omega). \tag{F6}$$

Since g_a is white noise of intensity μ_a, the equal-time variance is the integral of the corresponding power spectrum. The two terms in the numerator give the standard position and velocity contributions of the damped oscillator, $1/(2\mu_a)$ and $\tau_R/2$, respectively, and hence

$$\langle y_a^2 \rangle = \frac{\sigma_c^2}{2}(1 + \tau_R\mu_a). \tag{F7}$$

Substituting this result into Eq. (F5) and using both the orthogonality of $\mathcal{S}$ and $\mathcal{S}^T M \mathcal{S} = \widetilde{K}$ gives

$$\langle uu^T \rangle = \frac{\sigma_c^2}{2}(I + \tau_R\widetilde{K}). \tag{F8}$$

Transforming back to the original abundance fluctuations therefore yields

$$\Sigma = \langle \delta\mathbf{n}\, \delta\mathbf{n}^T \rangle = \frac{\sigma_c^2}{2}(N + \tau_R N\boldsymbol{\alpha} N). \tag{F9}$$

Forming the Pearson correlations from Eq. (F9) gives Eq. (27), with $\theta_i = \tau_R\bar{n}_i$. As $\tau_R \to 0$, the covariance becomes diagonal, recovering the matched-point Lotka-Volterra result and vanishing interspecific correlations.

We verified Eqs. (F9) and (27) against the numerical solution of the Lyapunov equation for the full $(S + Q)$-dimensional linear system in Eq. (F1). For random communities with heterogeneous $\bar{n}_i$, the two calculations agree to machine precision.

APPENDIX G: ADIABATIC ELIMINATION OF THE RESOURCES

This Appendix derives Eq. (28) and makes explicit the fast-resource reduction underlying the Lotka-Volterra description of Sec. II. We take the environment to act on the resources alone, $\sigma_c = 0$ and $\sigma_r > 0$ in Eq. (23), and eliminate the resources in the limit in which they are fast compared with the consumers.

Throughout the derivation, we exploit the separation of timescales. On the fast-resource timescale, the consumer abundances are treated as frozen parameters: The resource fluctuations are solved for these fixed abundances, and only after averaging over the fast process is the resulting effective white noise reinserted into the slow consumer dynamics.

1. Deterministic fast-resource reduction

Consider first the deterministic part of the consumer-resource dynamics. In the limit $\tau_R \to 0$, the resource variables relax to their instantaneous quasisteady values. On the positive-resource branch,

$$\bar{R}_k(\mathbf{n}) = 1 - \sum_i \lambda_{ki} n_i. \tag{G1}$$

Substituting Eq. (G1) into the consumer equation gives

$$\frac{dn_i}{dt} = n_i\left(r_i - \sum_j \alpha_{ij} n_j\right), \quad r_i = \sum_k \gamma_{ik} - 1, \quad \boldsymbol{\alpha} = \Gamma\Lambda. \tag{G2}$$

Thus, the deterministic fast-resource reduction retains the product $\Gamma\Lambda$ but not the separate yield and depletion matrices or the resource timescale.

2. Fast-resource fluctuations

Write $R_k = \bar{R}_k + \delta R_k$, with $\bar{R}_k(\mathbf{n})$ given by Eq. (G1).

Here, $\bar{R}_k(n)$ is the *instantaneous* quasisteady resource level corresponding to the current consumer abundances, which are regarded as constant during the fast-resource relaxation. On timescales short compared with the consumer dynamics, the abundances may be held fixed, and linearizing Eq. (23b) about $\bar{R}_k$ gives an Ornstein-Uhlenbeck process,

$$\tau_R \frac{d\,\delta R_k}{dt} = -\bar{R}_k\, \delta R_k + \sigma_r \bar{R}_k\, \zeta_k(t), \tag{G3}$$

with relaxation rate and stationary variance

$$\frac{1}{\tau_{\rm corr}} = \frac{\bar{R}_k}{\tau_R}, \quad \mathrm{Var}(\delta R_k) = \frac{\sigma_r^2 \bar{R}_k}{2\,\tau_R}. \tag{G4}$$

As τ_R is decreased the resource fluctuations become both faster and larger, and it is not obvious in advance, which of the two effects wins.

3. Effective white-noise intensity

A displacement δR_k changes the instantaneous per-capita growth rate of consumer i by

$$\delta\left(\frac{1}{n_i}\frac{dn_i}{dt}\right) = \sum_k \gamma_{ik}\, \delta R_k. \tag{G5}$$

The consumers are slow, so they do not resolve the shape of $\delta R_k(t)$, only its integrated effect: In the limit $\tau_R \to 0$ (but still $\sigma_r^2 \ll 2\tau_R\bar{R}_k$, so that the linearization remains controlled), each δR_k acts on them as a white noise whose *intensity* is

$$\mathcal{I}_k = 2\,\mathrm{Var}(\delta R_k)\,\tau_{\rm corr} = 2 \times \frac{\sigma_r^2 \bar{R}_k}{2\,\tau_R} \times \frac{\tau_R}{\bar{R}_k} = \sigma_r^2. \tag{G6}$$

This is the central step, and it settles the question the two effects raised. The increasing variance and the decreasing correlation time cancel exactly, leaving a finite white-noise intensity independent of both τ_R and the quasisteady resource level. No rescaling of the noise amplitude with the resource timescale is required, and the weights are uniform across resources, $\mathcal{I}_k = \sigma_r^2$ for every k.

4. Effective consumer-level forcing

Since the resources are uncorrelated [Eq. (25)], the effective consumer-level noise $\eta_i^{\rm eff}(t) = \sum_k \gamma_{ik}\, \delta R_k(t)$ has

covariance,

$$\left\langle \eta_i^{\rm eff}(t)\,\eta_j^{\rm eff}(t')\right\rangle = \left(\sum_k \mathcal{I}_k\,\gamma_{ik}\gamma_{jk}\right)\delta(t-t') = \sigma_r^2\,(\Gamma\Gamma^T)_{ij}\,\delta(t-t'), \tag{G7}$$

and the consumers obey a stochastic Lotka-Volterra system whose drift and diffusion matrices are

$$J = -N\boldsymbol{\alpha}, \quad \boldsymbol{\alpha} = \Gamma\Lambda, \quad D^{\rm eff} = N\,C^{\rm eff}\,N, \quad C^{\rm eff} = \sigma_r^2\,\Gamma\Gamma^T. \tag{G8}$$

The coarse graining therefore preserves the deterministic interaction matrix but replaces the environmental forcing by a different object. This separation is the mechanistic origin of the response-competition mismatch of the main text.

Two features distinguish $C^{\rm eff}$ from the Lotka-Volterra prescription of Sec. III, and together they are the sources of the mismatch. First, competition is built from the yield *and* the depletion, whereas the inherited forcing is built from the yield *alone*: The reduction preserves only the product $\Gamma\Lambda$, so a given niche-overlap matrix is compatible with a continuum of factorizations, and hence with a continuum of structural mismatches. For nonuniform forcing amplitudes, the relevant mismatch is $\Delta^{\rm eff} = C^{\rm eff} - Z$, with $Z = \frac{1}{2}(\boldsymbol{\alpha}H + H\boldsymbol{\alpha}^T)$, as in Eq. (31). When H is proportional to the identity, this reduces, after factoring out the common forcing amplitude, to the normalized mismatch $C^{(\eta)} - \boldsymbol{\alpha}_S$. Second, $C^{\rm eff}$ is not normalized to a unit diagonal: Its diagonal entries $\sigma_r^2\sum_k \gamma_{ik}^2$ differ from species to species, so a yield generalist, spreading its yield over many resources, inherits less environmental variance than a yield specialist.

A particularly important matched case is $\Lambda = c\,\Gamma^T$, with a common conversion factor c. Then, $\boldsymbol{\alpha} = c\,\Gamma\Gamma^T$, so the interaction and forcing structures are proportional. With the normalization $\alpha_{ii} = 1$, the diagonal of $\Gamma\Gamma^T$ is then uniform as well. This proportional relation is a sufficient condition for eliminating both sources of mismatch. It need not be necessary when $Q > S$, since components of Λ lying in the null space of Γ do not affect the product $\Gamma\Lambda$.

5. Numerical verification

The reduction is asymptotic, not exact, and must be checked. We integrated the full stochastic consumer-resource dynamics, Eq. (23) with $\sigma_c = 0$, directly in the Stratonovich convention, and compared the resulting pairwise abundance correlations with those of the reduced S-dimensional Lotka-Volterra system defined by Eq. (G8), holding σ_r *fixed* and applying no rescaling by τ_R. The comparison is shown in Fig. 6. The two descriptions agree pair by pair, which confirms Eq. (G6): With σ_r held constant, and with no compensating rescaling, the reduced system reproduces the full dynamics in the fast-resource limit.

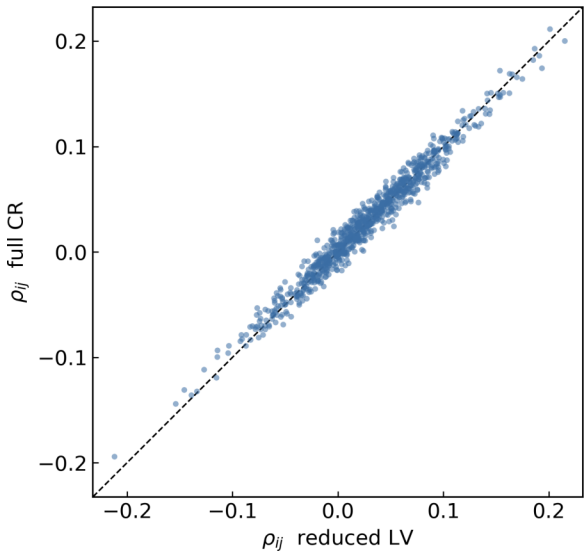


FIG. 6. The reduction is exact in the fast-resource limit. Pairwise abundance correlations from direct Stratonovich simulation of the full stochastic consumer-resource system, Eq. (23) with $\sigma_c = 0$, against those of the reduced Lotka-Volterra system with $\boldsymbol{\alpha} = \Gamma\Lambda$ and $C^{\rm eff} = \sigma_r^2\Gamma\Gamma^T$. The dashed line is the identity, and σ_r is the same in both descriptions with no rescaling by τ_R. Here, $S = 10$ consumers and $Q = 13$ resources. Parameters $\sigma_r = 0.02$ and $\tau_R = 0.05$. The plot shows the 45 pairs of each of 20 realizations. The Pearson correlation is 0.99 and the root mean square deviation from the identity is 0.01, the sampling error expected for a window of this length.

APPENDIX H: THE YIELD-DEPLETION MISMATCH

Section IV B identifies the quantity that acts as a source of abundance correlations under resource-mediated stochasticity as the weighted structural mismatch

$$\Delta^{\rm eff} = C^{\rm eff} - Z, \quad Z = \tfrac{1}{2}(\boldsymbol{\alpha}H + H\boldsymbol{\alpha}^T), \tag{H1}$$

where

$$C^{\rm eff} = \sigma_r^2\Gamma\Gamma^T, \quad H = \mathrm{diag}\left(C_{11}^{\rm eff},\ldots,C_{SS}^{\rm eff}\right), \quad \boldsymbol{\alpha} = \Gamma\Lambda. \tag{H2}$$

When the forcing amplitudes are common, $H \propto I$, this reduces after normalization to the mismatch $C^{(\eta)} - \boldsymbol{\alpha}_S$ of the main text.

Figure 4 is instead colored by the YDM of Ref. [13]. These are quantities of different origin: $\Delta^{\rm eff}$ is the exact Lyapunov source that determines the covariance, whereas YDM is a geometric predictor motivated by an exactly solvable two-species system. This Appendix defines YDM and gives its relation to $\Delta^{\rm eff}$, which is close but is not an identity. In Ref. [13], this quantity was denoted by D.

1. Definition of yield-depletion mismatch

Species i is characterized by two profiles across the resources: its yield $\gamma_i = (\gamma_{i1},\ldots,\gamma_{iQ})$, which says how much it gains from each resource, and its depletion $\lambda_i = (\lambda_{1i},\ldots,\lambda_{Qi})$, which says how much it removes. For a pair, the similarity of each profile is measured by its cosine, and the corresponding trait distance by

$$\Delta_{ij}^{\gamma} = 1 - \cos(\gamma_i,\gamma_j), \quad \Delta_{ij}^{\lambda} = 1 - \cos(\lambda_i,\lambda_j). \tag{H3}$$

The yield-depletion mismatch is defined via the difference

$$\mathrm{YDM}_{ij} = \Delta_{ij}^{\lambda} - \Delta_{ij}^{\gamma} = \cos(\gamma_i,\gamma_j) - \cos(\lambda_i,\lambda_j). \tag{H4}$$

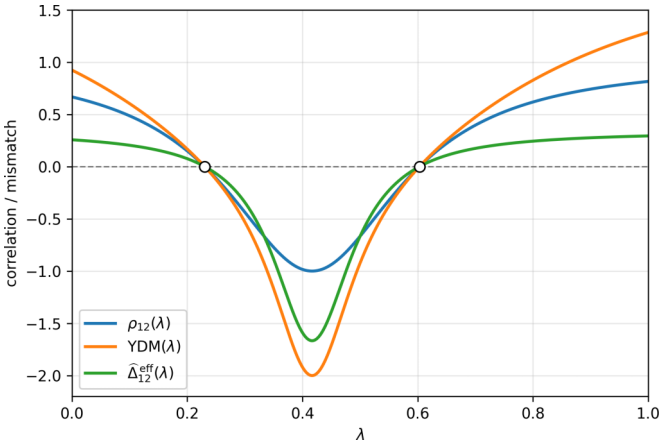


FIG. 7. Exact correlation, yield-depletion mismatch, and weighted matrix mismatch in the solvable two-species example. The exact abundance correlation $\rho_{12}(\lambda)$ of Eq. (H7), the yield-depletion mismatch YDM(λ) of Eq. (H8), and the normalized weighted mismatch $\widehat{\Delta}_{12}^{\rm eff}(\lambda)$ of Eq. (H11) are shown as functions of λ. The three quantities are not equal in magnitude, but have the same sign and cross zero at the same two values $\lambda_\pm = (5 \pm \sqrt{5})/12$, marked by the open circles. The exact Lyapunov mismatch and the geometrical YDM therefore encode the same qualitative transition in this analytically solvable case. At small and large λ, the two consumers draw their benefit from overlapping resources while depleting different ones, so YDM > 0 and the abundances are positively correlated, and between λ_- and λ_+ the relation is reversed.

It is positive when two species draw their benefit from the same resources but deplete different ones, negative in the reverse case, and zero when the two profiles are equally similar. This is the convention of Ref. [13], in which differences in yield generate negative correlations and differences in depletion generate positive ones, so that YDM and ρ_{ij} carry the same sign.

2. Relation to $\Delta^{\rm eff}$: related, but of different origin

$\Delta^{\rm eff}$ and YDM are not the same object. $\Delta^{\rm eff}$ is the exact Lyapunov source, while the correlations themselves reflect this source after propagation through the Lyapunov operator. YDM is instead a geometric predictor motivated by an exactly solvable two-species case [13].

To compare the yield-depletion mismatch with the exact dynamical mismatch $\Delta^{\rm eff}$, we revisit the exactly solvable two-consumer, two-resource example introduced in Appendix C of Ref. [13].

The yield and depletion matrices are chosen such that

$$\boldsymbol{\alpha} = \Gamma\Lambda = \begin{pmatrix} 1 & 2/3 \\ 2/3 & 1 \end{pmatrix}, \tag{H5}$$

with

$$\Gamma = \begin{pmatrix} \frac{6(2\lambda-1)}{12\lambda-5} & 2 - \frac{6(2\lambda-1)}{12\lambda-5} \\ \frac{4(3\lambda-1)}{12\lambda-5} & 2 - \frac{4(3\lambda-1)}{12\lambda-5} \end{pmatrix}, \quad \Lambda = \begin{pmatrix} \frac{5}{6} - \lambda & \lambda \\ \lambda & \frac{5}{6} - \lambda \end{pmatrix}. \tag{H6}$$

The exact abundance correlation is [13]

$$\rho_{12}(\lambda) = 1 - \frac{5}{15 + 12\lambda(6\lambda - 5)}, \tag{H7}$$

whereas the yield-depletion mismatch is

$$\mathrm{YDM}(\lambda) = 2 - \frac{2}{26 + 24\lambda(6\lambda - 5)} - \frac{50}{50 + 24\lambda(6\lambda - 5)}. \tag{H8}$$

For resource-mediated forcing, let

$$\tilde{Q} = \Gamma\Gamma^T, \quad \tilde{H} = \mathrm{diag}(\tilde{Q}_{11}, \tilde{Q}_{22}). \tag{H9}$$

(We write $\tilde{Q}$ rather than Q, since Q denotes the number of resources throughout the paper.)

The normalized weighted structural mismatch is

$$\widehat{\Delta}_{12}^{\rm eff} = \frac{\left[\tilde{Q} - \frac{1}{2}(\boldsymbol{\alpha}\tilde{H} + \tilde{H}\boldsymbol{\alpha}^T)\right]_{12}}{\sqrt{\tilde{Q}_{11}\tilde{Q}_{22}}} = \frac{\Delta_{12}^{\rm eff}}{\sqrt{C_{11}^{\rm eff} C_{22}^{\rm eff}}}, \tag{H10}$$

with $\tilde{Q} = \Gamma\Gamma^T$ and $\tilde{H} = \mathrm{diag}(\tilde{Q})$, so that $C^{\rm eff} = \sigma_r^2 \tilde{Q}$ and $H = \sigma_r^2 \tilde{H}$. The common factor σ_r^2 therefore cancels between numerator and denominator, so $\widehat{\Delta}_{12}^{\rm eff}$ does not depend on the noise amplitude. For the matrices above, this becomes

$$\widehat{\Delta}_{12}^{\rm eff}(\lambda) = \frac{2(36\lambda^2 - 30\lambda + 5)}{3(72\lambda^2 - 60\lambda + 13)}. \tag{H11}$$

The three quantities are not identical, but they have the same sign and vanish at the same two values,

$$\lambda_\pm = \frac{5 \pm \sqrt{5}}{12}. \tag{H12}$$

Thus, in this exactly solvable example (Fig. 7), the geometrical proxy YDM(λ) and the weighted matrix mismatch $\widehat{\Delta}_{12}^{\rm eff}(\lambda)$ identify the same changes in the direction of the abundance correlation, although their magnitudes differ.

[1] A. Goyal, L. S. Bittleston, G. E. Leventhal, L. Lu, and O. X. Cordero, Interactions between strains govern the eco-evolutionary dynamics of microbial communities, eLife **11**, e74987 (2022).

[2] M. Sireci, M. A. Muñoz, and J. Grilli, Environmental fluctuations explain the universal decay of species-abundance correlations with phylogenetic distance, Proc. Natl. Acad. Sci. USA **120**, e2217144120 (2023).

[3] K. Crocker, A. Skwara, R. Kannan, A. Murugan, and S. Kuehn, Timescale of environmental change modulates metabolic guild cohesion in microbial communities, ISME J. **19**, wraf186 (2025).

[4] X. Chen, K. Crocker, S. Kuehn, A. M. Walczak, and T. Mora, Inferring resource competition in microbial communities from time series, PRX Life **3**, 023019 (2025).

[5] J. Camacho-Mateu, A. Lampo, M. Sireci, M. A. Muñoz, and J. A. Cuesta, Sparse species interactions reproduce abundance correlation patterns in microbial communities, Proc. Natl. Acad. Sci. USA **121**, e2309575121 (2024).

[6] M. Loreau and C. de Mazancourt, Biodiversity and ecosystem stability: A synthesis of underlying mechanisms, Ecol. Lett. **16**, 106 (2013).

[7] E. H. van Nes, D. G. F. Pujoni, S. A. Shetty, G. Straatsma, W. M. de Vos, and M. Scheffer, A tiny fraction of all species forms most of nature: Rarity as a sticky state, Proc. Natl. Acad. Sci. USA **121**, e2221791120 (2024).

[8] M. Kalyuzhny, R. Kadmon, and N. M. Shnerb, A neutral theory with environmental stochasticity explains static and dynamic properties of ecological communities, Ecol. Lett. **18**, 572 (2015).

[9] P. Chesson, Species competition and predation, in *Ecological Systems*, edited by R. Leemans (Springer, New York, NY, 2013), pp. 223–256.

[10] J. W. Spaak and F. De Laender, Intuitive and broadly applicable definitions of niche and fitness differences, Ecol. Lett. **23**, 1117 (2020).

[11] M. Barbier, J.-F. Arnoldi, G. Bunin, and M. Loreau, Generic assembly patterns in complex ecological communities, Proc. Natl. Acad. Sci. USA **115**, 2156 (2018).

[12] J. Camacho-Mateu, A. Lampo, S. Ares, and J. A. Cuesta, Nonequilibrium microbial dynamics unveil a new macroecological pattern beyond Taylor's law, Phys. Rev. E **110**, 044402 (2024).

[13] A. Goldberg, O. Shtossel, Y. Louzoun, and N. M. Shnerb, Niche overlap is not enough: Same overlap, contrasting fluctuations, Ecol. Lett. **29**, e70425 (2026).

[14] J. Sakarchi and R. M. Germain, MacArthur's consumer-resource model: A Rosetta stone for competitive interactions, Am. Nat. **205**, 306 (2025).

[15] E. Postma, C. Verduyn, W. A. Scheffers, and J. P. Van Dijken, Enzymic analysis of the Crabtree effect in glucose-limited chemostat cultures of *Saccharomyces cerevisiae*, Appl. Environ. Microbiol. **55**, 468 (1989).

[16] J. D. Bjørge, J. Overgaard, H. Malte, N. Gianotten, and L.-H. Heckmann, Role of temperature on growth and metabolic rate in the tenebrionid beetles *Alphitobius diaperinus* and *Tenebrio molitor*, J. Insect Physiol. **107**, 89 (2018).

[17] M. Basan, S. Hui, H. Okano, Z. Zhang, Y. Shen, J. R. Williamson, and T. Hwa, Overflow metabolism in *Escherichia coli* results from efficient proteome allocation, Nature (London) **528**, 99 (2015).

[18] J. R. Speakman, Body size, energy metabolism and lifespan, J. Exp. Biol. **208**, 1717 (2005).

[19] J. A. Vucetich, R. O. Peterson, and C. L. Schaefer, The effect of prey and predator densities on wolf predation, Ecology **83**, 3003 (2002).

[20] N. Owen-Smith, *Megaherbivores: The Influence of Very Large Body Size on Ecology* (Cambridge University Press, Cambridge, 1988).

[21] P. A. Jansen, F. Bongers, and L. Hemerik, Seed mass and mast seeding enhance dispersal by a Neotropical scatter-hoarding rodent, Ecol. Monogr. **74**, 569 (2004).

[22] L. M. Gosling and S. C. Roberts, Scent-marking by male mammals: Cheat-proof signals to competitors and mates, Adv. Study Behav. **30**, 169 (2001).

[23] Y. Liu, J. Hu, and J. Gore, Ecosystem stability relies on diversity difference between trophic levels, Proc. Natl. Acad. Sci. USA **121**, e2416740121 (2024).

[24] T. Gibbs, Y. Zhang, Z. R. Miller, J. P. O'Dwyer, and J. Grilli, Stability criteria for the consumption and exchange of essential resources, PLoS Comput. Biol. **18**, e1010521 (2022).

[25] E. Blumenthal, J. W. Rocks, and P. Mehta, Phase transition to chaos in complex ecosystems with nonreciprocal species-resource interactions, Phys. Rev. Lett. **132**, 127401 (2024).

[26] D. A. Kessler and N. M. Shnerb, Generalized model of island biodiversity, Phys. Rev. E **91**, 042705 (2015).

[27] G. Bunin, Ecological communities with Lotka-Volterra dynamics, Phys. Rev. E **95**, 042414 (2017).

[28] Y. Fried, D. A. Kessler, and N. M. Shnerb, Communities as cliques, Sci. Rep. **6**, 35648 (2016).

[29] R. West and N. M. Shnerb, Quantitative characteristics of stabilizing and equalizing mechanisms, Am. Nat. **200**, E160 (2022).

[30] O. S. Venturelli, A. V. Carr, G. Fisher, R. H. Hsu, R. Lau, B. P. Bowen, S. Hromada, T. Northen, and A. P. Arkin, Deciphering microbial interactions in synthetic human gut microbiome communities, Mol. Syst. Biol. **14**, MSB178157 (2018).

[31] T. E. Gibson, Y. Kim, S. Acharya, D. E. Kaplan, N. DiBenedetto, R. Lavin, B. Berger, J. R. Allegretti, L. Bry, and G. K. Gerber, Learning ecosystem-scale dynamics from microbiome data with MDSINE2, Nat. Microbiol. **10**, 2550 (2025).

[32] P. L. Nguyen, F. Pomati, and R. P. Rohr, Inferring coexistence likelihood in changing environments from ecological time series, Proc. Natl. Acad. Sci. USA **122**, e2417905122 (2025).

[33] R. R. Stein, V. Bucci, N. C. Toussaint, C. G. Buffie, G. Rätsch, E. G. Pamer, C. Sander, and J. B. Xavier, Ecological modeling from time-series inference: Insight into dynamics and stability of intestinal microbiota, PLoS Comput. Biol. **9**, e1003388 (2013).

[34] J. Grilli, Macroecological laws describe variation and diversity in microbial communities, Nat. Commun. **11**, 4743 (2020).